Geothermal Resource Group, Inc.
77530 Enfield Lane, Building E
Palm Desert, CA 92211
Phone: 760-341-0186

Akutan Geothermal: Resource Report

Upper Hot Springs Bay Valley, Fumarole Area, geothermal surface manifestation

This material is based upon work supported by the U.S. Department of Energy's Office of Energy Efficiency and Renewable Energy (EERE) under the Geothermal Technologies Office Award Number DE-EE0000329.

15 May 2019

Contents

Executive Summary

Geothermal energy resources are present in the Hot Springs Bay Valley geothermal area, and the City has invested considerable money and time in the exploration of the resource for future use. Exploration activities funded primarily through a grant the City was awarded from Alaska Energy Authority and later supplemented by the U. S. Department of Energy (DOE), with cost share from the City. The exploration led to the development of a geothermal resource conceptual model that was built and refined between 2008 and 2018. During this period, geological and geophysical studies, exploration drilling and other activities were completed, including a preliminary feasibility study for a power project, investigations of the terrain for suitability for access and development, environmental and archeological review, plus TG well abandonment and a review of economic considerations.

The model of the resource predicts that there is a viable geothermal resource in two general areas: on the northwest edge of Hot Springs Bay Valley going northwest of the valley (hot springs area) and southwest of the Valley (fumarole area). The resource temperature for the valley area is expected to be about 170°C (340°F) and given the size and permeability estimates (with a factor for the level of confidence in the estimates), the mean power capacity of the outflow resource is 3 MWe and the P50 (most likely) power capacity is 1 MWe. The fumarole area has an expected resource temperature of 240°C (464°F) and given the size and permeability estimates mean capacity is 20 MWe and the P50 (most likely) capacity is 9 MWe.

Permeability is the most difficult factor to predict and has a significant impact on the available geothermal fluids and therefore the amount of power that can be generated. The uncertainty in this value is the main reason for lower confidence in the likelihood of exploration success and the wide range in predicted MW values. The permeability has been difficult to locate as indicated by the results of the flow test at AK-3 in 2017. The test resulted in the production of some fluid, but due to low permeability, the recharge to the wellbore was too slow to sustain flow.

The greatest probability of overall MWe production is in the fumarole region, but development is hampered by poor accessibility. The extremely high cost of road building for exploratory drilling, put an end to planning at an intermediate stage of the project and refocused attention on the viability of development in the hot spring outflow part of the resource.

The City will be determining what the next steps are with AK-3, which is still that is still open and maintained in a suspended status in HSBV. While AK-3 remains accessible (not plugged with cement) it will need to be maintained. The City has a bond with AOGCC that will remain in place until the well is abandoned. GRG recommends that the well be maintained open as an asset for the foreseeable future.

Next Steps

- Determine short term plan for AK-3
    - Location survey and wellhead inspection required
    - Abandon in 2019 not recommended
    - Maintain for future use
        - Currently under suspension approved until 2020
        - Inspection required
        - Likely that the well will be needed in the time frame of its viability
- Revisit Fumarole exploration plan
    - Budgetary estimates for access, drilling and testing to prove resource
    - Feasibility given new economic development in City
    - Sketch development plan
- Define possible development scenarios for hot springs site
- Identify interested developers
- Identify additional grant opportunities

Introduction

The City of Akutan has pursued development of a geothermal resource on Akutan for energy production since 2008, exploration and confirmation of the resource has progressed as possible with seasonal limitations for field work and funding agency requirements. Akutan was initially a prospective target for geothermal development as it is formed by an active volcano, and has surface manifestations of the geothermal energy, the resource developed with the circulation of heat provided by the volcano, through natural fractures in the rock. Continued work has confirmed that there is a geothermal resource available in the Hot Springs Bay Valley (HSBV) geothermal area.

Akutan has the opportunity to become a center of commerce and industry for the Aleutian chain, now with a harbor at the head of Akutan Bay and an airport on the adjacent Akun Island (Figure 1). The largest land based seafood processing facility in North America is also located here. With the support of the City of Akutan, the geothermal prospect area has been extensively studied, including geophysical surveys (magnetotelluric and gravity), geological mapping, geochemical studies, and drilling of three small diameter wells, two in 2010 and one in 2016. Work on the scenarios for development of the resource has also been completed, including infrastructure needed for power generation, transmission and maintenance, and financial feasibility. Some of this is now several years old but retains significance in terms of magnitude of needed expenditures for development and project feasibility.

The primary exploration area through this work was on HSBV floor where surface manifestations of geothermal heat include hot springs and a geyser located along the northeast edge of the valley. A secondary area, generally referred to as the fumarole site, is located at approximately 1500' elevation in the western part of the field. Though the indications of a higher temperature geothermal resource exist in this area, the higher cost of exploration, drilling, and development of this site were not justified for energy required to meet the island's electricity demand. As a result, the fumarole area development has not been pursued to confirmation.

Figure 1: View from helicopter coming into Akutan Bay from HSBV. Harbor development foreground, Trident fish processing plant on left middle ground, City is adjacent to plant, airport located on Akun island in distance.

Akutan Corporation is the owner of surface property rights to the project site and The Aleut Corporation owns the subsurface. Both Corporations have executed binding agreements providing the City of Akutan full control of the property for purposes of geothermal resource exploration and development. The City is also designated as the managing partner for the Akutan Corporation and Tribal Council for purposes of receiving and administering project funds. Funding for geothermal resource exploration and evaluation, including test well drilling, were from a State of Alaska Renewable Energy Grant Fund grant in the amount of $2,595,000. The grant was for a three-phase project from State of Alaska Renewable Energy Grant Fund, with cost share by the City of Akutan. The first phase was to do initial studies and geoscience in order to complete a prefeasibility study and target exploration wells, Phase 2 was slated to comprise exploration well drilling, and Phase

3 was for project design. The project activities evolved somewhat from the original plan as new data influenced the decisions regarding next steps. The City worked with AEA to ensure that new activities were following the grant objectives. Additional funds were garnered during Phase 3 of the project through a novation process of the U.S. Department of Energy bringing $931,000 originally allocated for geothermal exploration on neighboring Makushin Island to the City of Akutan, which allowed for the drilling and testing of the third temperature gradient hole in HSBV in 2016/2017.

The generalized exploration history for geothermal development since 2008:

- 2009-Initial field exploration, development of initial conceptual model of the field, prefeasibility study
- 2010-Drilling TG-2 and TG-4, data interpretation, refinement of conceptual model of field, feasibility study
- 2012-2013-Additional field surveying for deep drilling at fumarole site (geologic mapping, geophysical surveys), conceptual model update, targeting and initiation of planning for deep drilling and site development
- 2013-Abandonment of first two thermal gradient holes in HSBV
- October 2013-Start of Phase 3-Planning for feasibility of development of geothermal project based at Fumarole area (design project including access roads, drilling, plant and pipelines, budgeting)
- 2014-Request for project rescoping to reevaluate the development of the Hot Springs site due to high project cost at fumarole site
- September 2014-Secure DOE funding that allows for drilling of additional thermal gradient well
- 2015-2016-Project re-scoping, budgeting, well targeting, drilling and testing planning
- August-September 2016-Drilling AK-3
- August 2017-Flow test AK-3

This report serves to summarize the exploration and findings to date, update the conceptual model of the geothermal resource, and provide a geothermal resource estimate.

A key turning point in the project came as Phase 3 was proceeding. The results of the drilling of TG-2 and HSBV-4 (thermal gradient wells to ~1000ft) in the valley floor, indicated a very shallow hot resource, but the wells were not tested, and it was concluded that the shallow resource would be susceptible to degradation once producing. The conceptual model indicated that the fumarole manifestation may indicate the “upflow” area where a deeper, hotter fluid would be circulating. Since most of the data prior to drilling data was collected to assess the characteristics of the

resource in the HSBV itself and to target the TG wells, there was limited data from the surrounding terrain, that could show the characteristics of the upper valley and potential geothermal system structure underlying the fumarole area. The 2012 campaign was designed to collect more data from the surrounding area in order to further develop the conceptual model and to be able to target exploration wells at the fumarole area. Following this fieldwork and subsequent conceptual model updates, AEA granted permission for the project to move into Phase 3.

In the original conception of the project, Phase 3 would encompass preparation of a development plan. The plan was to include engineering, design, and environmental documents necessary to proceed to permitting and construction. The proposed plan was to include cost estimates for the major project elements such as production drilling, road and infrastructure development, plant construction, and operation and maintenance costs over the 20-year life of the project. This was to be used to perform an economic assessment and business plan. Fieldwork conducted in 2013 focused on the data collection and resource evaluation needed for project design and cost estimating. The work also included an environmental analysis to evaluate project impacts and determine permitting requirements.

A project scoping meeting was held in Las Vegas, Nevada in October 2013, wherein several subcontractors were assigned tasks for the preparation of the development plan. A review was scheduled at that time. At the review meeting, high level budget estimates for the implementation of the project as it was being designed, were higher than expected, and the City of Akutan (led by RMA) determined that it was not worthwhile to continue the development document to completion. A project suspension was implemented, and the City requested an opportunity to rescope the project to use the remaining project funds for different activities than originally assigned. AEA approved the request and subsequently funding from DOE became available through a novation process bringing funding from a geothermal project on Makushin to the Akutan Geothermal Project. The rescoped project included the drilling and testing of an additional well in the HSBV, to search deeper than the original two wells, and also to perform well testing that was not planned or done on the previous two wells. The drilling and testing completed the explorations activities to be funded under the original AEA grant. The resource conceptual model developed as a result of all the work completed through the project will serve as the basis for future development or continued exploration of the project.

Previous Conceptual Model(s) – 2009-10

Two conceptual models of the Akutan Geothermal Resource were developed by Kolker et al. (2010) prior to any drilling, both of which describe the HSBV geothermal system as a single resource with a high temperature (>500 °F / >240 °C) upflow zone located at depth somewhere

proximal to the fumaroles, and a lower-temperature outflow aquifer (~360-390°F / 180-200°C) that daylights as the hot springs in HSBV. The difference between the two endmember conceptual models is with alternative outflow pathways as either along the L-shaped path of HSBV, or along a northern trajectory around Mount Formidable from the fumaroles to the hot springs (Figure 2 and Figure 3). These model variances on outflow were initially preferred because the flow paths followed major structural features identified or inferred from the surface maps available at the time. Subsequent data collection, analysis and integration between 2011 and 2018 was used to update and refine these models including geophysics, geology, geochemistry, drilling, core analyses, well testing, and model updates based on this work.

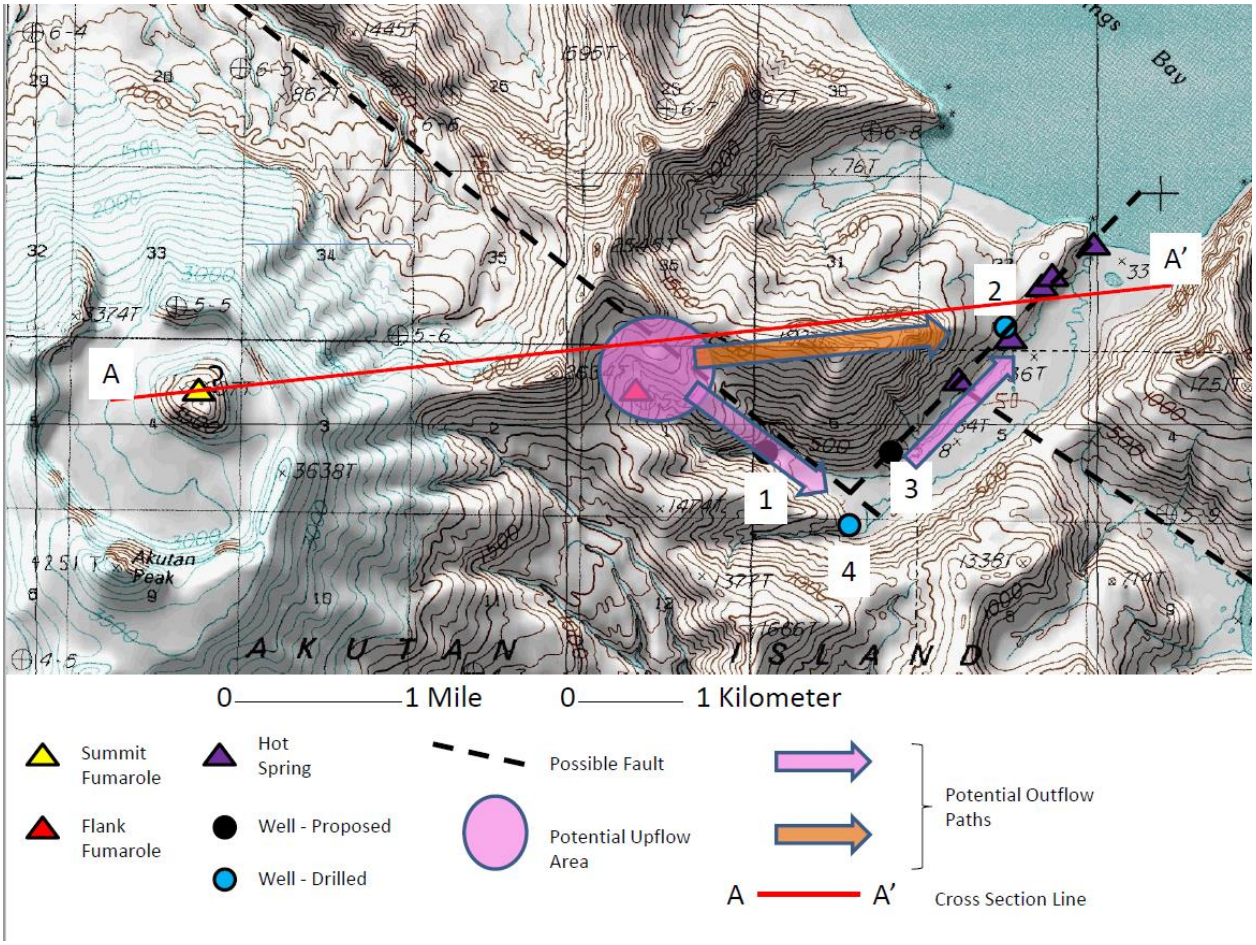

Figure 2: Map view of early conceptual model of HSBV geothermal resource showing potential flow paths from the fumarole area to the hot spring area, locations of first TG wells drilled in 2010 shown. Results of 2011 drilling confirmed south side of valley location of TG-4 is out of the influence of the shallow outflow path.

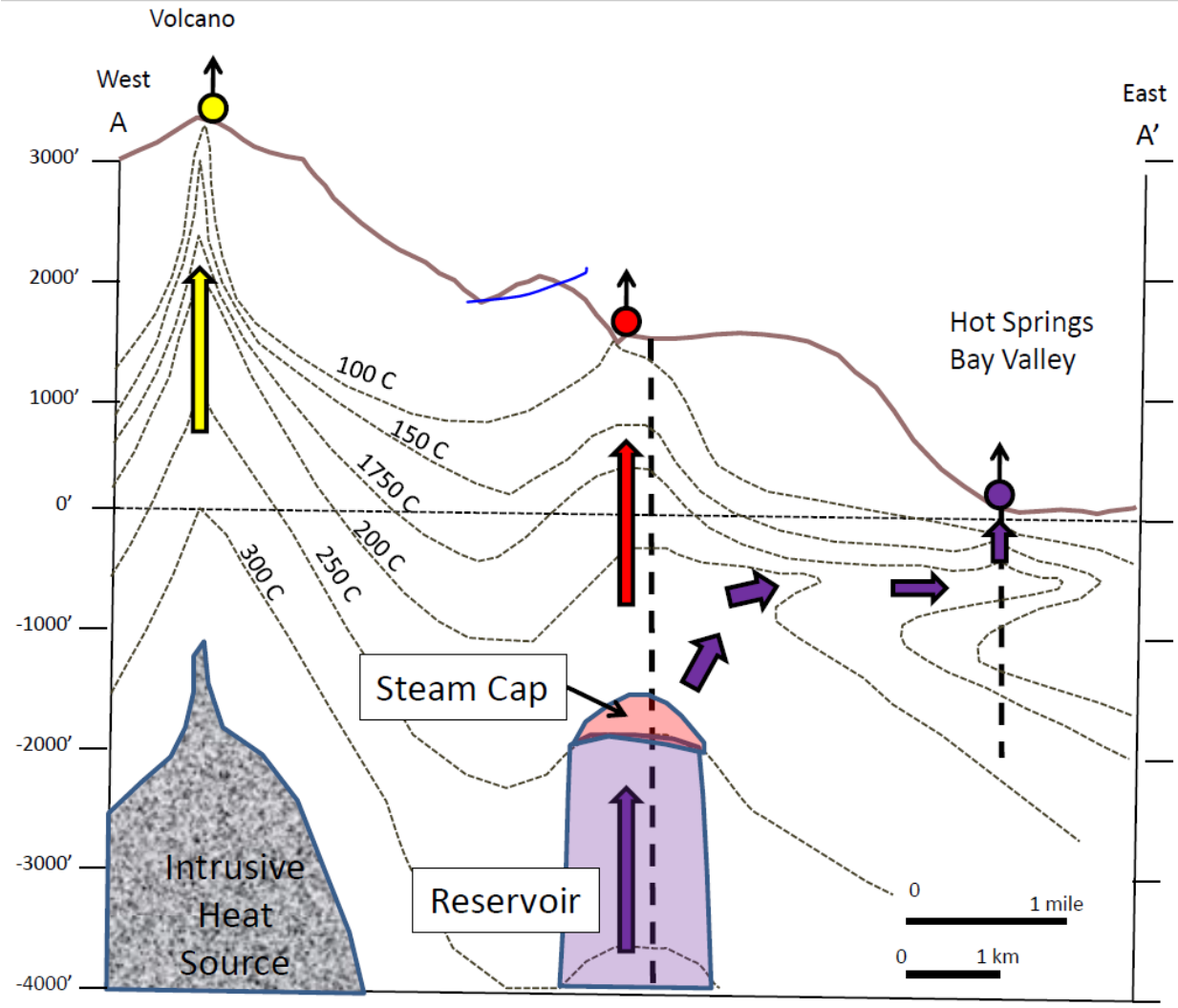

Figure 3: Cross section from original conceptual model for HSBV geothermal resource, showing temperature patterns based on inferred flow paths affected by an intrusive heat source.

Expanded Surface Studies – 2012

A field season in 2012 comprised the bulk of new data collection after the drilling of the first two wells, activities included:

- Expansion of Magnetotelluric (MT) survey coverage to include the inferred primary upflow area under the fumarole field
- Collection of gravity data along with MT survey to assess variation in reservoir rocks (e.g., intrusive versus extrusive stratigraphic units) for possible joint 3D inversion

- Conduct details surface geology mapping of stratigraphy, structure, alteration and surface manifestations – detailed mapping not previously conducted.

More detail on these activities is given below.

Geology-Surface Mapping and Structural Analysis

Detailed geologic mapping and structural analyses were conducted in August 2012. Approximately 15 sq. mi. (25 km^2) were mapped, including all of HSBV, the upper half of Long Valley, and along the northeastern flank of Akutan volcano (Hinz and Dering, 2012). Key results of the new mapping include: 1) adding substantial detail to the fault mapping within the geothermal area and across the island, 2) obtaining kinematic and dip information for many of the faults, 3) completing the first detailed mapping of the alteration, 4) mapping previously undiscovered hot springs and fumaroles (Figure 4 and Figure 5Figure 5).

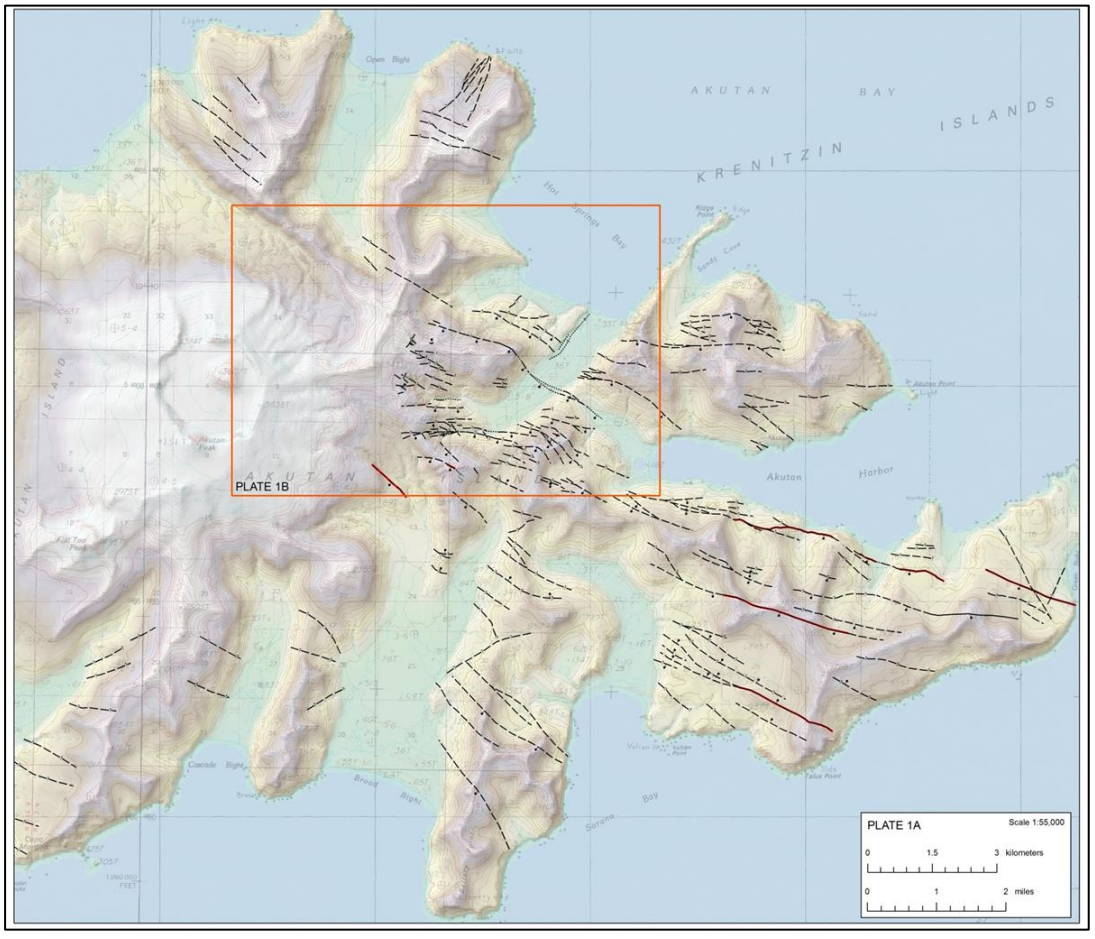

Figure 4: Fault map of Akutan Island (Hinz and Dering, 2012).

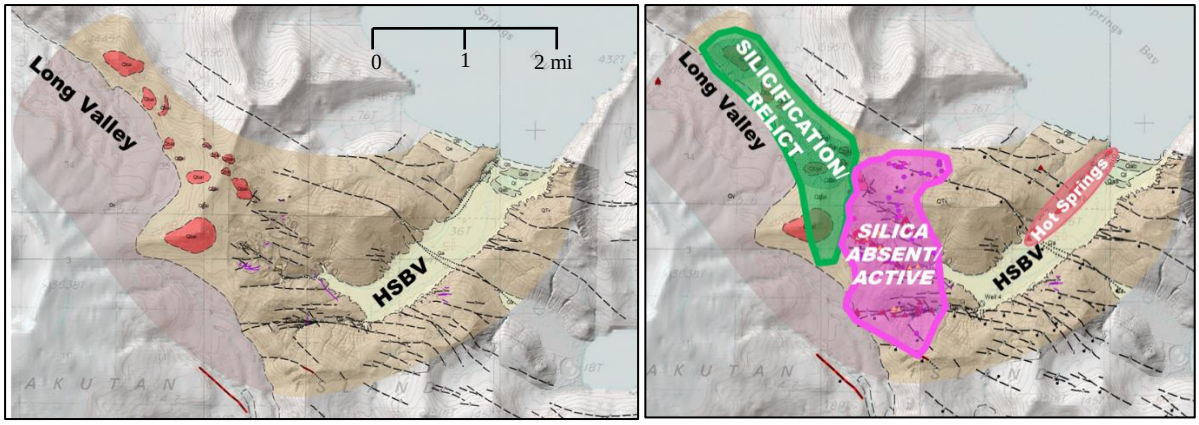

Figure 5: Geologic map of HSBV and Long Valley (Hinz and Dering, 2012) on left, compared with areas of alteration highlighted on right.

This mapping built on existing stratigraphic studies (Motyka et al., 1991; Romick, 1993; Richter et al., 1998). The older consolidated rock into which HSBV was carved consists of interbedded basaltic and andesitic lava flows, ash fall tuff layers, and mass wasting deposits, as observed in the valley walls as well as in the drill core from both TG-2 and TG-4.

Hot Springs Bay Valley was named for the several dozen hot springs present in the lower portion of the valley. The hot springs occur in a narrow (100 m wide) linear band at the base of the NW valley wall that extends ~1 mile (1.5 km) from the midpoint of the lower valley to the sea (Figure 6). Within the band, hot springs are clustered into five groups, A–E and range from 54 to 94 ºC, with springs located further up-valley generally having higher temperatures.

At the head of the upper portion of HSBV is a vigorous fumarole field covering an area of ~85,000 sq ft (~26,000 m^2) composed of four large and dozens of smaller individual gas vents measured at 99–100 ºC at 1,370 feet (417 m) elevation (Figure 7). The larger fumarole vents are roughly linearly aligned to the NE, as is a large boiling mud pot that appeared between 1996 and 2009 and doubled in diameter between 2010 and 2012 to ~15 m diameter (Kolker et al., 2012; Stelling, pers. Comm., 2012). There is also a lone fumarole in the drainage below the main cluster (Figure 8).

Faults in HSBV range from < 0.6 to 6 miles (1 to 10 km) strike length, with <65 ft (20 m) of stratigraphic offset. These structures can be classified into three groups, one striking E-W, one NE-SW, and one WNW-ESE (Figure 9). The faults are a combination of normal, oblique slip, and strike-slip motion observed across all groups. Overall, Akutan is in a transtensional setting, which is good for providing overall structurally enhanced stratigraphic permeability. However,

individual faults are relatively small with little offset, and therefore have a low probability for providing major permeability zones. No major faults capable of deep circulation were observed in HSBV.

Hydrothermal alteration in HSBV consists of argillic alteration surrounding surface expression of fluid flow, especially in the fumarole area where intense alteration has created hazardous conditions. Significant argillic alteration exists in the bottoms of the east-west trending tributary valleys at the head of HSBV. Alteration around the hot springs is minor and limited in extent to the perimeter of each spring. Long Valley, northwest of HSBV, contains significant relict argillic alteration with significant silicification.

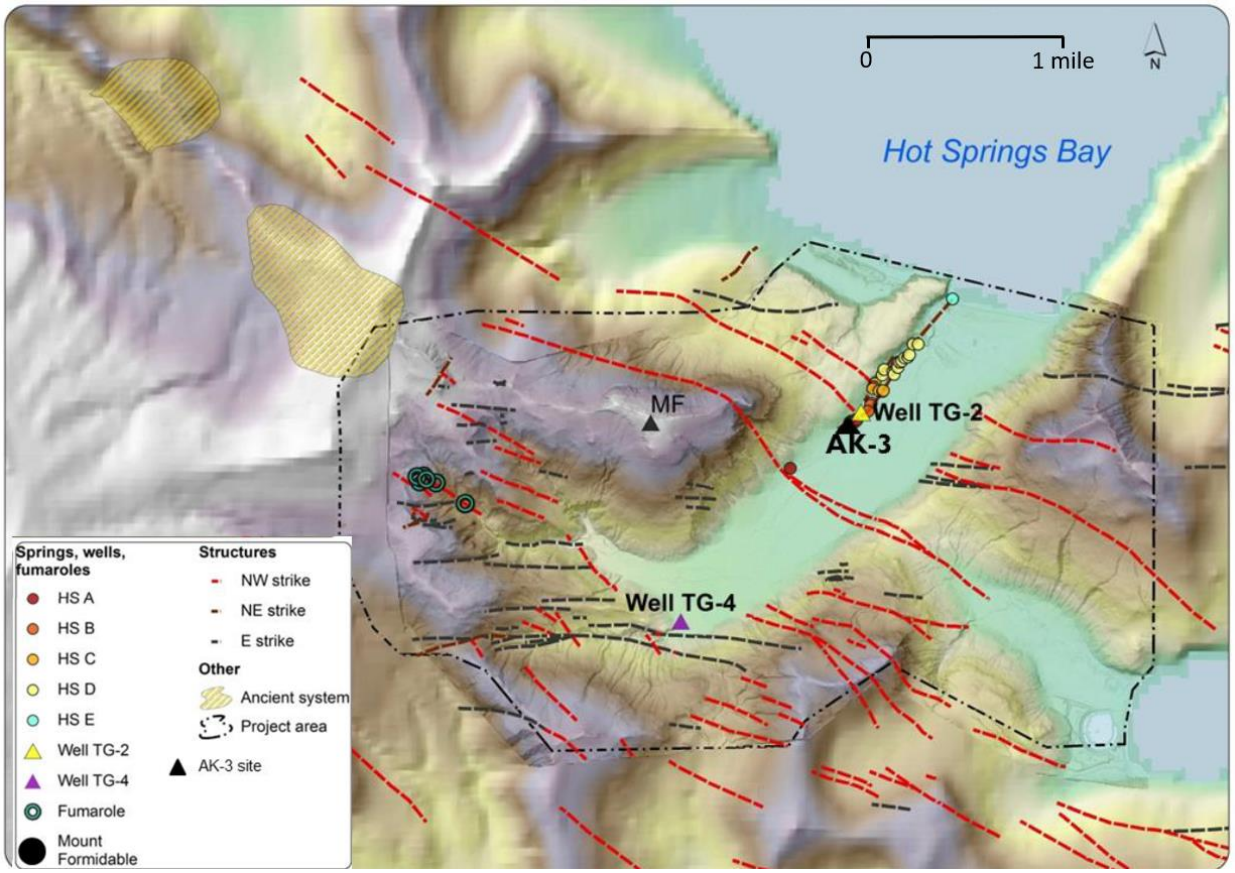

Figure 6: Distributions of geothermal surface manifestations, explorations wells within HSBV geothermal area.

Figure 7: Upper part of fumarole field viewed from north.

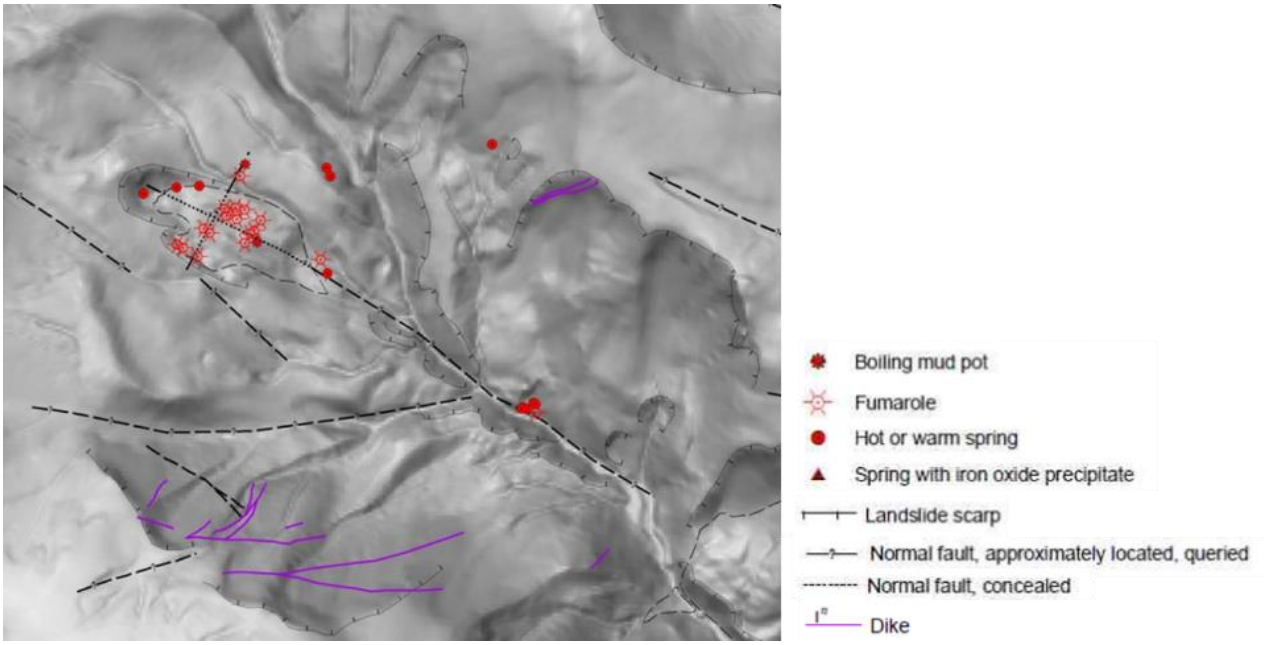

Figure 8: Close up of fumarole field map (Hinz and Dering, 2012)

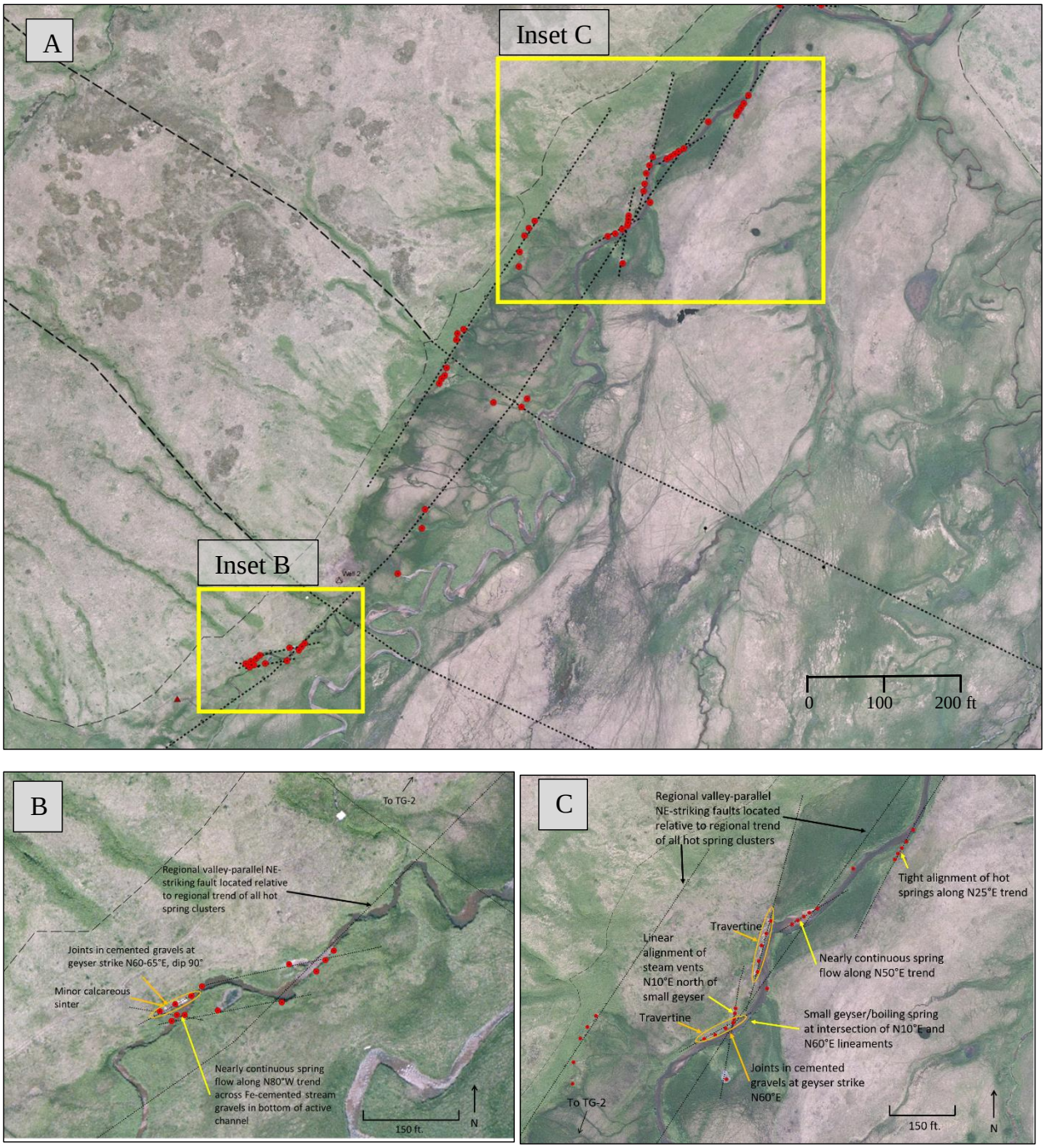

Figure 9: Distribution of hot springs in lower HSBV.

Magnetotelluric (MT) Survey

In 2012, a second, 46-station MT survey was conducted to complement the initial 52-station survey of 2009. The 2012 survey expanded the project area to the west to include the area west of the fumarole area and to fill in gaps. The combined data set was used to create a non-traditional 3D model by first creating 2D inversions along point to point, fence-diagrams. These were stitched together to create a 3D representation of the MT resistivity. Although this approach conveys a 3D interpretation of the subsurface resistivity, it is not 3D inversion modeling. The current model was clipped to 6,562 ft. (2000 m) below sea level to remove deeper, less reliable inversion results. Horizontal smoothing was applied to the model in order for the model to more easily predict the shallow resistivity values between widely spaced stations. Therefore, abrupt changes in shallow resistivity between stations are blurred, and steeply dipping structures (e.g., faults, or other high angle contacts between units) are not reliably resolved in the geophysical model.

Overall, the HSBV area is lacking the <10 ohm-m signatures typical of many productive geothermal systems. Although a very low resistivity (1–10 ohm-m) zone near the hot springs is present at relatively shallow depths (surface – ~150 ft. (50 mFigure 10), with higher resistivity values at greater depth, this unit is not very thick or widespread. A moderately-low resistivity unit (10–40 ohm-m) is present across most of the modeled area, particularly in the upper portion of HSBV (Figure 10). This shallow conductive layer has an average thickness of ~820 ft (250 m; maximum 1640 ft (500 m)), and forms a rough antiformal structure plunging gently to the northeast from the inferred upflow beneath the fumaroles to the outflow hot springs (Figure 10). The southern limb of this antiform extends to the margin of the main valley, and the northern limb thins to the NNE and is absent at the northern margin of the study area. This layer of moderately low resistivity could be the result of an immature clay cap, partial erosion of an older clay cap, or a laminated outflow interlayered with relatively high permeability (and therefore more readily altered) lithologies bracketed by lower permeability units, resulting in a higher overall resistivity signature. The drill core contains altered ash fall layers with elevated permeability surrounded by lower permeability lava flow units, supporting the idea of a lithologically constrained outflow sheet. Additionally, mineralogical evidence from the core shows high-temperature alteration minerals present at surprisingly shallow depths, indicating there may have been significant erosion of the clay cap. However, surface exposures of alteration near the upflow are argillic, rather than propylitic, suggesting that any erosion of the clay cap has been incomplete, and some clay cap remains.

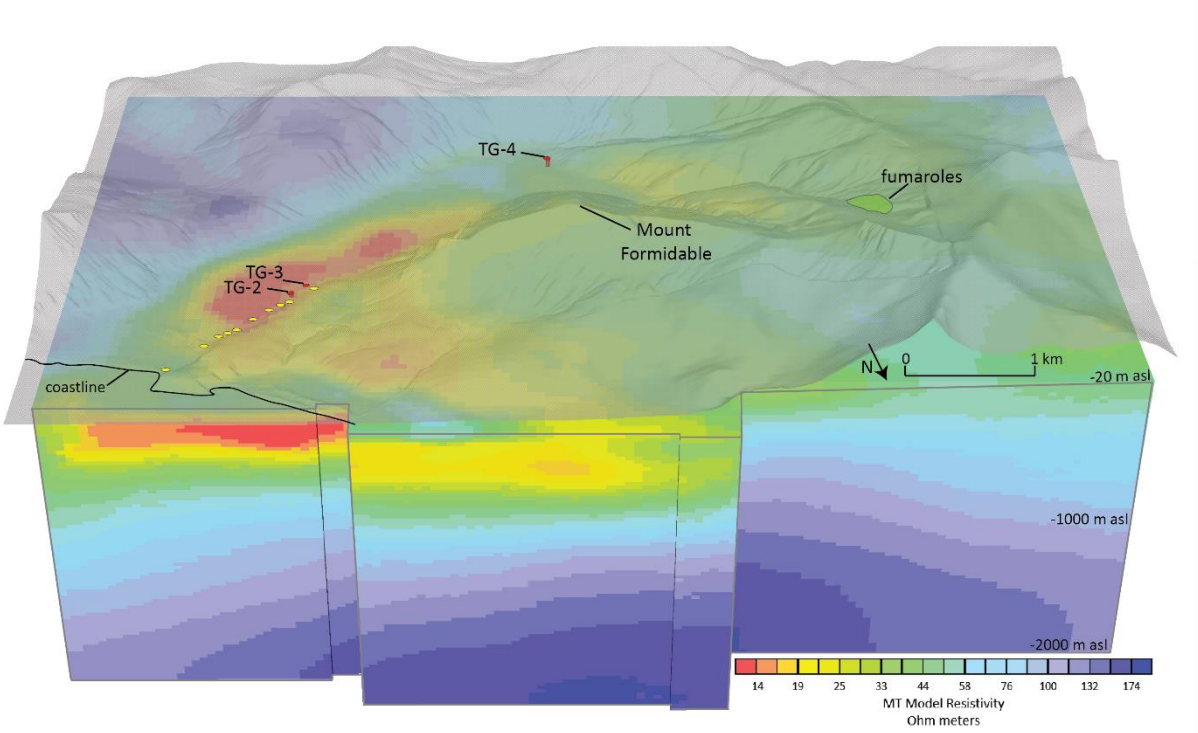

Figure 10: Integrated 2009 and 2012 MT results, view to SSW. Top surface is topography, and labels point to surface features and expressions; yellow ovals are generalized hot spring locations. The 30-40 ohm m iso-resistivity surfaces (green) extend from beneath the fumaroles beneath Mount Formidable in a general antiform structure. Lower resistivity patterns are observed along the main trend of HSB Valley and along the coastal flank of Mount Formidable. The <14 ohm-m iso-resistivity regions (red) occurs only near the hot springs and at deeper levels beneath the coastal bench. Top of MT data truncated at 20 m below sea level.

Gravity

A gravity survey was conducted in 2012, concurrent with the MT survey. A pseudo-basement surface was created from the gravity data assuming an average density of 2.33 g/cm^3. Figure 11 shows elevation contours on this pseudo- basement surface, with colors representing the MT resistivity model slice at 300 m below sea level. Although the exact values of the pseudo-basement contours depend on the assumed rock densities, the shape and gradient of the contours reveal dense elongate body that extends from the ridge between upper Broad Bight Valley and HSBV northeast beneath Mount Formidable, suggesting higher densities in this area (Figure 11). The high density of this feature suggests it is low porosity and therefore relatively unaltered and is likely an intrusion or series of basaltic intrusions. The gravity data is consistent with MT results and surface features as well, aligning with the northwest margin of the conductive zone and the northwest valley margin (e.g., in line with the chain of hot springs in the lower HSBV). This linear expression has been

interpreted to be structurally controlled, and it is possible that the emplacement of small intrusions at depth are also structurally controlled.

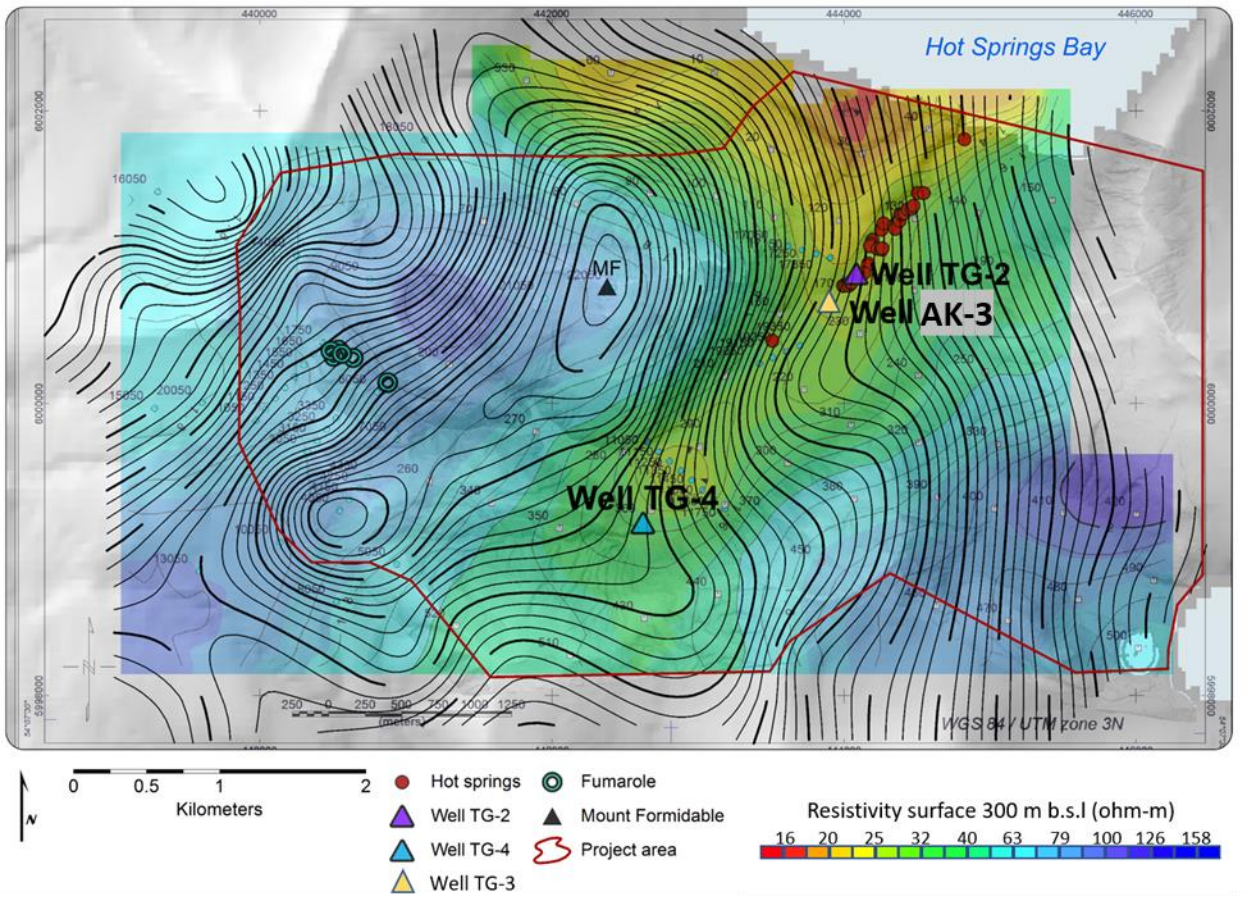

Figure 11: Map view of MT resistivity at 300 m below sea level (colored background; see legend), with gravity pseudo-basement depth contours superimposed. Gravity modeled assuming a density of 2.33 g/cm3 (contour interval 25 m, heavy contours every 100 m). Note the isolated gravity highs beneath MF and beneath the ridge south of the HSBV fumaroles. Small gray boxes are 2009 MT stations; small light blue circles are 2012 MT stations. Figure from Stelling et al., 2015.

Geochemistry

Fluid and gas samples have been collected from various locations on Akutan by a variety of investigators. There are published fluid geochemical data from hot springs, meteoric water and fumarole gases (Motyka and Nye, 1988; Motyka et al., 1993; Symonds et al., 2003a, b). Several samples have been gathered during exploration work including water samples collected during drilling of TG-2 and TG-4 and the well test of AK-3. The chemistry indicted from work to date is that of a mature neutral-chloride reservoir brine and geothermometry indicates equilibrium

temperatures above 200°C (390°F). The temperature has been confirmed by downhole temperature measurements in AK-3.

A sample from the productive zone in TG-2 at 584 feet (178 m) depth was collected during drilling in 2010; one was collected from the bottom of TG-2 (833 ft; 254 m depth); and one from TVD in TG-4 (1500 ft; 457 m depth). Of the three well samples from the first two thermal gradient wells, two were slightly contaminated with drilling fluid (TG-4 1500 ft. and TG-2 833 ft), and one sample (TG-4 1500 ft.) was contaminated through air lift to the surface. The well discharge sample from TG-2 at 584 ft. (178 m) appears uncontaminated. The sample collected from AK-3 testing in 2017 showed a lack of evidence for equilibrium with rock at elevated temperatures, negative charge imbalance, dissimilarity with other thermal waters. These are indicators that the water sample AK-3a is not representative of a subsurface thermal aquifer and therefore evaluation of this water will probably not provide evidence of an underlying geothermal reservoir. Low Mg and HCO_3, as well as higher δ Oxygen-18 and δ Deuterium than typical meteoric waters, indicate AK-3a is also not a meteoric water. The conclusion is that this fluid may have been condensate, as there was limited permeability at AK-3 and the well could not sustain flow, but fluid was discharged for a short time when the well was allowed to heat up, which could result in condensation within the heated wellbore as it recovered.

Fluid samples from the hot springs and well discharge confirm that the hot springs represent a neutral-chloride reservoir brine. Chlorine concentrations are significantly lower in hot springs samples than in the TG-2 well discharge sample, indicating near-surface dilution by meteoric water (Table 1). Cation concentrations in Akutan liquids show a linear trend between the sample from TG-2 (584 ft; 178 m) and meteoric fluid, further supporting significant near-surface mixing of hydrothermal and meteoric water. Mixing with meteoric water in and near HSBV also explains the overall dilute chemistry of the spring water and well production fluids. The uncontaminated sample from TG-2 (584 ft; 178 m), which has slightly elevated Mg concentrations relative to TG-2 (833ft; 254 m), suggests slightly more mixing with meteoric water than found in the deeper sample. These samples represent reservoir brines with modest meteoric dilution, and the true reservoir fluids could be nearer the equilibration curve with temperatures between 230°C and >240°C, indicating a relatively mature reservoir (Figure 12).

Table 1: Laboratory analysis of AK-3 (sample AK-3A) and No Name Spring. SiO2 for AK-3A is corrected for dilution. The publicly available data for regional waters HS A3, HS B1, HS C4, HS D2, HS E, Fum Sp, TG-2 and TG-4 included from Stelling et al. (2015); the cold water samples AKU12-15, AKU12-16, AKU12-18, AKU12-19, AKU12-20, AKU12-21 included from (U.S.G.S., Scientific Investigations Report 2013-5231, 2012).

Well/Site	Sampling Temp-erature	Lab pH	Reported Brine Data																	
			TDS	Na	K	Ca	Li	Mg	Sr	As	B	SiO_2	HCO_3	SO_4	Cl	F	Fe	NH4	CO_3	Mn
	°C		mg/kg																	
AK-3A	100.0	8.28	558	310	22	68	0.38	<0.5	0.74	0.03	37	14	18	23	64	0.3	0.02	0.5	<1.0	0.12
No Name Spring	92.2	7.40	2400	740	71	110	2.30	19.0	1	1.5	31	120	86	31	1200	<10	0.74	1.1	<1.0	0.37
HS A3	84.0	7.00		323	28	12	1.30	0.9			11	145	172	43	420	1.1				
HS A3	84.0			328	26	12	1.20	1.0			12	135		41	410	0.9				
HS B1	47.4	6.40		172	16	15	0.61	1.5			5.9	103	116	22	220	0.6				
HS C4	73.4	6.50		207	16	18	0.61	1.6			7	133	118	43	280	1.0				
HS D2	58.8	6.80		128	9	11	0.34	12.0			3.4	91	128	26	140	0.9				
HS E	67.0	7.30		1660	74	130	1.10	320.0			4.5	121	161	495	3440	0.5				
Fum Sp	92.3	2.60		17	4	32	0.01	13.0				220		1300	5.2					
TG-2, 178m	182.0	6.72		693	69	15	1.72	0.4			50	219	152	55	1048	1.2				
TG-2, 254m	171.0	7.95		876	104	292	2.03	0.3			27	314	26	70	1872	1.0				
TG-4, 500m	163.0	8.11		420	115	2751	0.75	1.7			6	37	22	32	5745	0.7				
AKU12-15	5.3	7.49	42	3	0	5	<0.001	0.9				7	16	6	4	0.0	0.04			0.02
AKU12-16	10.5	6.86	172	33	3	12	0.08	2.0				21	35	7	58	0.1	0.35			0.1
AKU12-18	5.8	7.02	47	4	0	6	<0.001	1.0				8	18	5	4	0.0	0.03			0.02
AKU12-19			14	4	1	1	<0.001	0.5				0		1	7	0.0	0.03			0.03
AKU12-20	5.7	6.71	53	9	1	10		2.1				15		3	13	0.0	0.33			0.08
AKU12-21														6	12	0.1				

Na/K, Na-K-Mg diagram and the silica mixing diagram all suggest that the source fluids of the Akutan thermal waters could be above 200 °C. No Name spring appears to be conductively cooled. Mixing plots indicate the other hot springs (besides HS-E) are cooled through mixing with meteoric waters. The mixing for the other hot springs could have occurred in the immediate area of the springs. No Name Spring does not follow the same mixing trend as the other hot springs, suggesting cooling by conduction could occur as a result of lateral outflow from the geothermal source of temperature greater than 200 °C (Figure 13).

One spring in the fumarole area was sampled (Fum Sp in Table 1) which contained much more sulfur, lower total dissolved solids and had a lower pH than springs associated with the outflow near the mouth of HSBV. The fumarole spring sample also contained higher SiO_2 than the outflow fluids, which is likely caused by boiling of ascending upflow fluids beneath the fumaroles. These compositions highlight the differences in fluid type between the upflow (fumaroles) and outflow (hot springs).

Six fumarole gas samples (gas and condensate samples for three separate features) were also collected in 2012, all of which appear to be of high quality. Gas geochemistry of the fumaroles from the head of HSBV and from the summit of Akutan Volcano indicate these are two separate systems. The summit fumaroles have relatively low CO_2 content and inconsistent data (Figure 14), indicative of gas release above an acidic core (Giggenbach, 1987). In contrast, the consistency of the HSBV fumarolic gas data suggest these samples come from a relatively well equilibrated reservoir. Additionally, because the Y-values of these data plot above the lower boundary, it is

likely that some fraction of gas is derived from equilibrated steam, indicating the presence of a localized steam cap in the reservoir (Giggenbach and Glover, 1992).

Updated liquid geothermometer calculations (Powell and Cumming, 2010) were applied to both published chemical analyses of Akutan hot spring waters (Motyka and Nye, 1988; Bergfeld et al., 2014) as well as recently collected hot spring, fumarole gas and condensate, and well discharge fluids. Table 2 presents the results of several cation and silica geothermometers. Figure 12 is a graphical representation of the Na–K–Mg geothermometer (Giggenbach and Glover, 1992). Because dilution through mixing with meteoric water is likely, these compositions have been extrapolated to the equilibrium line, suggesting temperatures of at least 230°C, and likely exceeding 240°C. If the sample from TG-2 (833 ft; 254 m) is only modestly contaminated by drilling fluid and reflects the dilution path, the projected temperature could be closer to 260°C.

Silica geothermometers, which tend to record more recently equilibrated fluid temperatures, yield temperatures of ~170 °C for TG-2 (584 ft; 178 m), agreeing with the spring chemistry interpretations of Motyka and Nye (1988) and Symonds et al. (2003a,b), and with the maximum measured well discharge temperature of 182 °C. This is consistent with a higher temperature (>240 °C) source that is capable of producing an outflow aquifer with temperature ~180 °C, consistent with the hot spring and borehole production cation and silica geothermometry (Table 2). Geothermometry estimates from HSBV fumarole gases consistently suggests reservoir temperatures of 270–300 °C, as shown, for example, on a HAR–CAR plot (Figure 14). Samples that plot outside this cluster appear to have variable influence from atmospheric gas (Kolker et al., 2012; Bergfeld et al., 2014).

As indicators of subsurface temperatures, SiO_2-based geothermometers are reduced by mixing, especially when mixed with cold meteoric water in hot and warm spring samples. A plot of SiO_2 versus measured temperature for available hot spring and well data was used to develop a trendline beyond the available data to predict the concentration of SiO_2 in equilibrium with quartz in the reservoir, and provide an approximate estimate of reservoir temperature (Figure 15). The extrapolated trendline indicates silica is approximately 343mg/kg in the reservoir, which suggests a reservoir temperature of about ~220°C (applying the quartz conductive cooling geothermometer to the hot end-member concentration). The quartz geothermometer applied to the silica concentration TG-2 sample from 178 m which is most directly representative of subsurface conditions (measured temperature 182°C; Stelling, 2015) indicated a temperature of ~180°C.

Both the cation geothermometers and silica mixing diagram suggest that the temperatures of the thermal source of TG-2 and No Name Spring could be above 200°C possibly as high as 230 °C. If the No Name spring is diluted to achieve the current discharge chemistry, as suggested by the cation trilinear, it could be that it was originally a more concentrated brine than TG-2 (178 m). No

Name spring appears to be conductively cooled. Mixing plots indicate the other hot springs (besides HS-E) are cooled through mixing with meteoric waters. The mixing for the other hot springs could have occurred in the immediate area of the springs. No Name Spring does not follow the same mixing trend as the other hot springs, suggesting cooling by conduction could occur as a result of lateral outflow from the geothermal source which could be >200 °C.

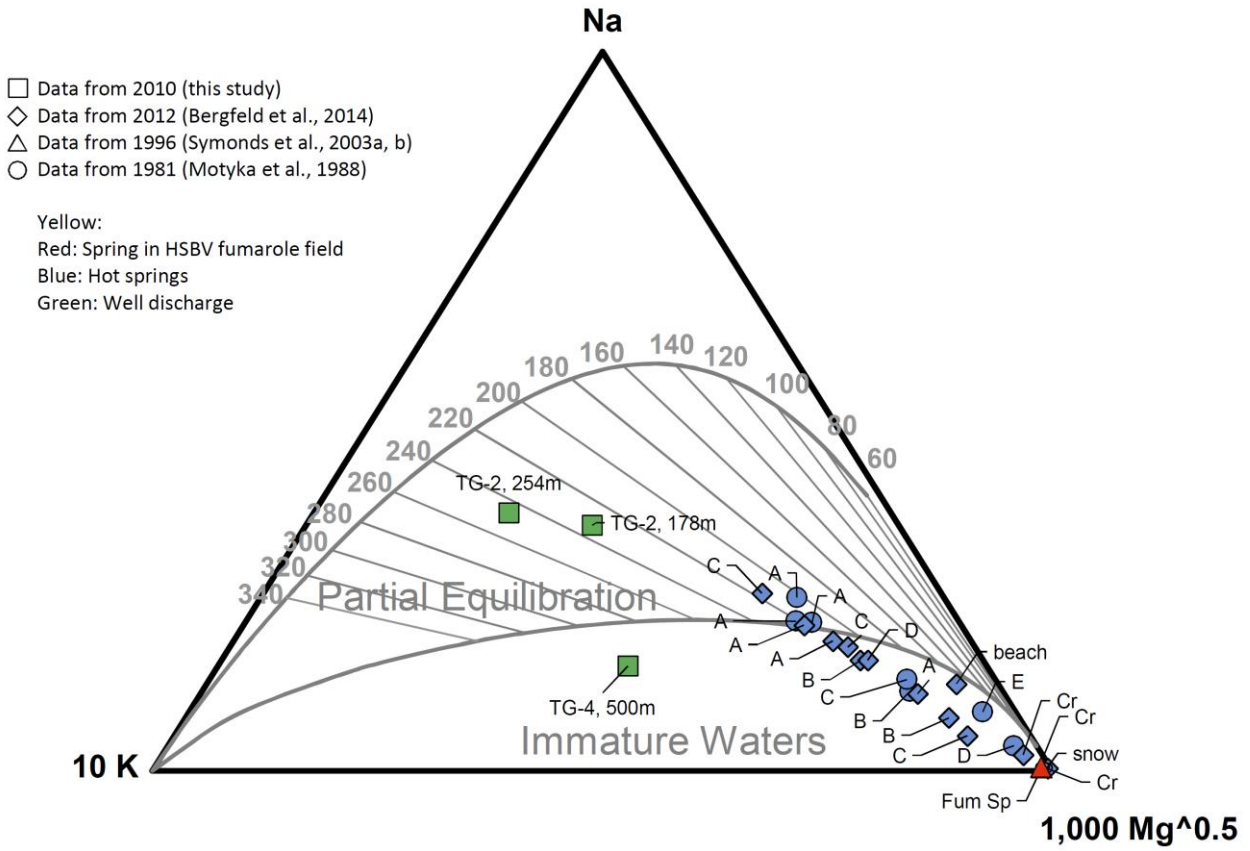

Figure 12: Na–K–Mg ternary diagram for Akutan hot springs and well discharge samples. Letters refer to hot spring groups from Motyka et al., (1993; A is further up-valley, E is at the coast). Fum Sp = spring in HSBV fumarole field; Cr = creek above hot springs. Varying extent of partial equilibration for all samples suggests dilution along the flow path. Extrapolation from hot springs lineaments and the discharge from TG-2: 178 m indicate deep reservoir temperatures of at least 220–240 ◦C. Geothermometry of the deeper sample from TG-2 and the sample from TG-4 should be discounted due to contamination with drilling fluids. Plot made using program from Powell and Cumming, 2010.

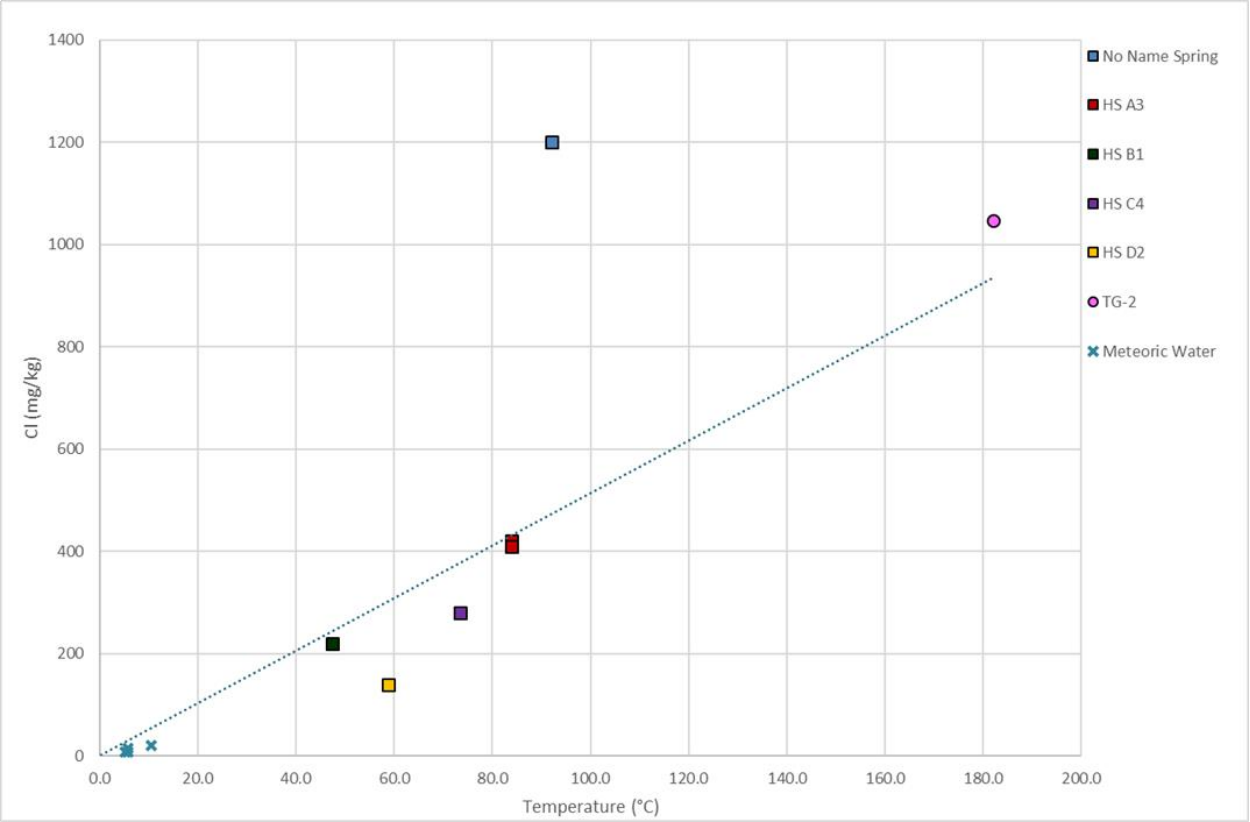

Figure 13: Mixing is shown between all samples aside from No Name Spring. No Name Spring has similar concentrations of Cl as TG-2 (178m), indicating that both are composed of the same geothermal fluid, but the fluid at No Name Spring has undergone conductive cooling. HS E was omitted as it had mixed with seawater, resulting in elevated Cl concentrations. TG-2 (254m) and TG-4 chemistry is repetitive, and therefore not included.

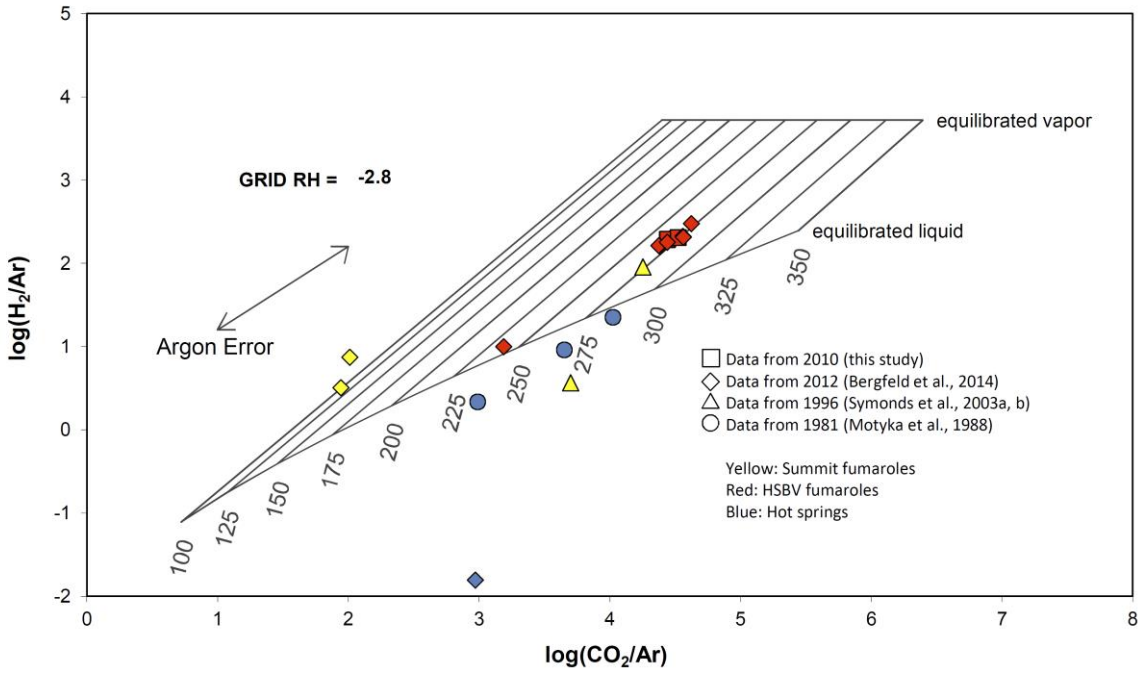

Figure 14: HAR–CAR plot of gas geochemistry. Samples collected in 2010 are consistent and have values that plot within the grid, suggesting a component of equilibrated steam. Geothermometry ranges from 260 to 275°C. RH value (oxidation state) of −2.8 is typical for an equilibrated geothermal system associated with an andesitic stratovolcano (Giggenbach, 1991). Plots generated using algorithms of Powell and Cumming (2010).

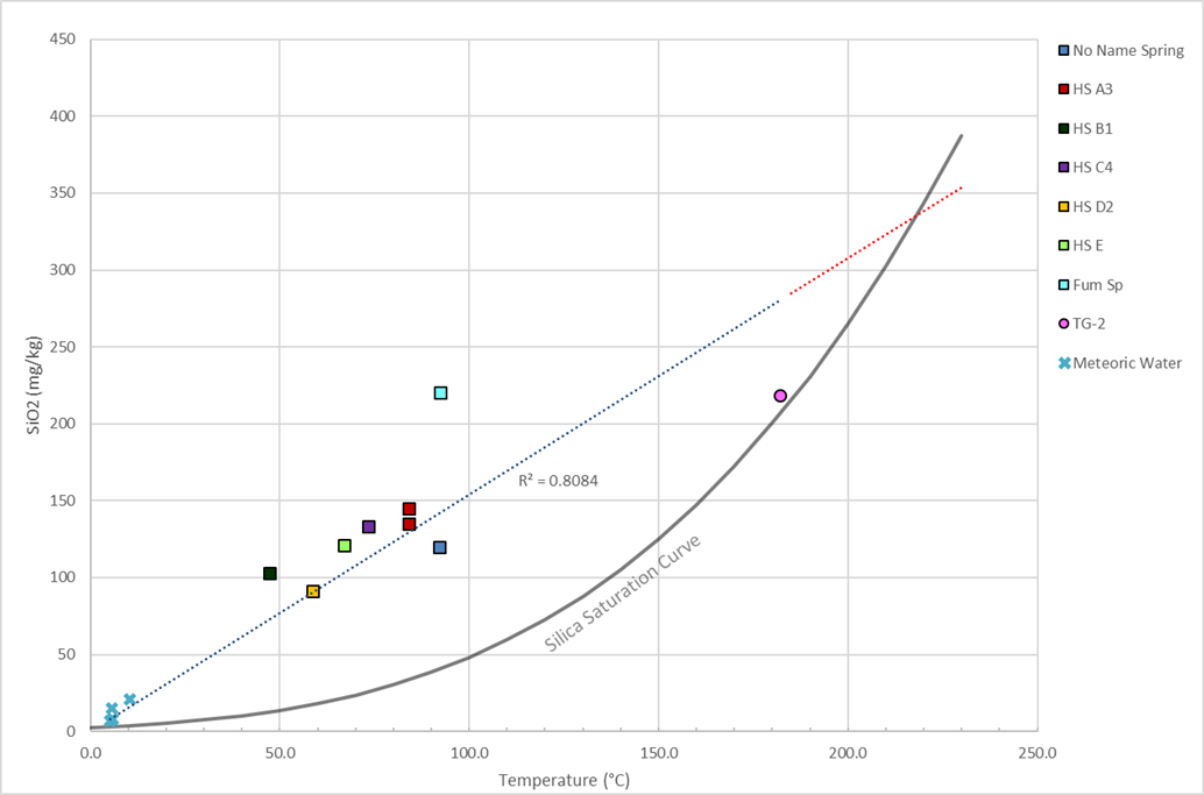

Figure 15: The dissolved silica concentration of the various hot springs and cold meteoric water is plotted, yielding a mixing line of geothermal and non-geothermal fluids, shown as the blue line. Extrapolation of this line can be used to determine the temperature of geothermal fluid before mixing. The silica saturation curve is plotted in black and intercepts the mixing line at a silica concentration of 343mg/kg. This silica concentration corresponds with a reservoir temperature of 220°C using the Quartz conductive cooling geothemometer model (Fournier 1982).

Table 2: Geothermometry results for Akutan hot springs and discharge waters. Calculations from spreadsheets by Powell and Cumming (2010).

Sample	Chalcedony cond	Quartz cond	Na-K-Ca	Na-K-Ca Mg corr	Na/K Fournier	Na/K Truesdell	Na/K Giggenbach	K/Mg Giggenbach
HS A3	135	159	189	148	205	173	221	127
HS A3	130	155	185	136	198	164	214	123
HS A3*	133	157	178	140	186	149	203	125
HS B1	112	139	179	97	211	180	227	103
HS C4	129	154	171	99	196	161	213	102
HS D2	105	132	164	-245	191	156	208	64
HS E	123	148	162	-349	156	114	175	74
Fum Sp	166	187	40	-103	288	281	297	42
TG-2-178	166	187	211	211	217	187	232	173
TG-2-254	197	214	196	196	232	207	246	198
TG-4-500	58	89	87	87	322	329	328	165

Drilling, Well Tests, Core Data

Three exploration wells have been drilled in HSBV, the first two (TG-2 and TG-4) in 2010 and AK-3 in 2016. Well targets, well design, depth, diameter and testing options for all three were influenced and limited by the accessibility limitations into HSBV, environmental concerns with wetlands and streams, water accessibility and the significant terrain between the valley floor and the fumarole area. All three were drilled with the Major LF 90 core rig, chosen for its small size and ability to be broken down and moved by a reasonably sized helicopter. AK-3 was selected to test as deep as possible to intersect faults that may be carrying geothermal fluids to the surface. A deeper hot resource in this lower part of the valley could be attractive for development, if viable, as compared to the shallow outflow resource that interacts too easily with the surface waters or the deeper resource inferred to exist in the fumarole area, which is less accessible. The AK-3 well was also planned to be tested, unlike the first two wells that were drilled as thermal gradient wells, though TG-2 did encounter a thermal reservoir that flowed from about 585 ft. In AK-3 this shallow zone was anticipated and cased through in order to drill into a potential deeper reservoir.

Geothermal Gradients in TG wells

During drilling, TG-2 encountered high geothermal gradient with a peak in well fluid temperature between 587-583 ft (178 and 179 m) depth at a highly permeable zone that vigorously flowed 359°F (182°C) geothermal fluid (Figure 16). In order to drill and test deeper formations, this zone was cemented and cased off before flow-rate measurements could be conducted. Due to a host of complications during drilling, many stemming from the unexpectedly high temperature at shallow depth, TG-2 was terminated at 833 ft. (254 m), approximately half the planned total depth.

Well TG-4, located at the southwestern corner of the intersection of the two HSB valleys, was drilled to the planned 1,500 ft. (~500 m) depth. As expected of a well located just outside the margins of an outflow, no significant water flow was encountered in TG-4 and indications of high permeability were not encountered below ~213 ft (65 m). Steep geothermal gradients were observed, asymptotically approaching an isothermal temperature of 163°C (Figure 17), suggesting that, although the well is outside the main upflow or outflow, it is being conductively heated from a nearby geothermal reservoir.

Well AK-3, located ~200 meters up-valley from TG-2 encountered a fracture at 165 ft where the well flowed, but the shallow permeability is inconsequential for the geothermal development. The well was cased to 800 ft, though there were permeability indicators between 700 and 800 feet, the potential deeper reservoir was the target of the third well. The hottest part of the well is at about 400 ft depth at 357°F, with a declining temperature profile below, indicating a hot water entry shallow, interpreted to be horizontal permeability as is found in the outflow part of the geothermal system (Figure 18). The well was able to flow only intermittently, with minimal recharge from the open hole section between 800 and 1000 ft.

The equilibrated temperature profile in TG-2 (Figure 16) shows two zones of steep geothermal gradients in the upper half of the well: 6°F/100ft (110°C/km) from 20 to 118 ft. (6 to 36 m), and up to 25°F/100ft (460°C/km) from 118 to 400 ft. (36 to 122 m), beyond which temperature begins to stabilize. This may reflect a narrowed zone of near-surface lateral fluid flow beginning at 114 ft (35 m) depth. The zone of apparent sharp cooling in the end-of-well profiles is the result of addition of drilling fluid and cement into the productive zone at 584 ft. (178 m) in order to preserve borehole integrity after it flowed. The equilibrated temperatures profile indicates the permeable zone has recovered and records the hottest equilibrated temperatures (338°F; 170°C). Note that the equilibrated temperature at 584 ft. (178 m) is 53°F (12°C) cooler than flowed water temperatures measured during drilling, suggesting that the 359°F (182°C) fluid was being "pulled in" laterally from a nearby region of limited volume. In the interval between the maximum equilibrated temperatures and total vertical depth (TVD; 833 ft.; 254 m) a modest temperature reversal (~40°F; ~5°C) is present, suggestive of convective heating from a localized layer of migrating fluid.

Temperature profiles in TG-4 (Figure 17) show similar steep geothermal gradients in the shallow portions of the well (750°C/km from 82 to 164 ft. (25 to 50 m), and 240°C/km from 164 to 591 ft. (50 to 180 m) depth, below which temperatures gradually stabilize and become nearly isothermal at 323°F (162°C) between 984 and 1394 ft. (300 and 425 m). Although permeable zones

were not encountered in this well, the isothermal gradient below 984 ft. (300 m) suggests the rock body is being convectively heated by fluid flow within a nearby reservoir.

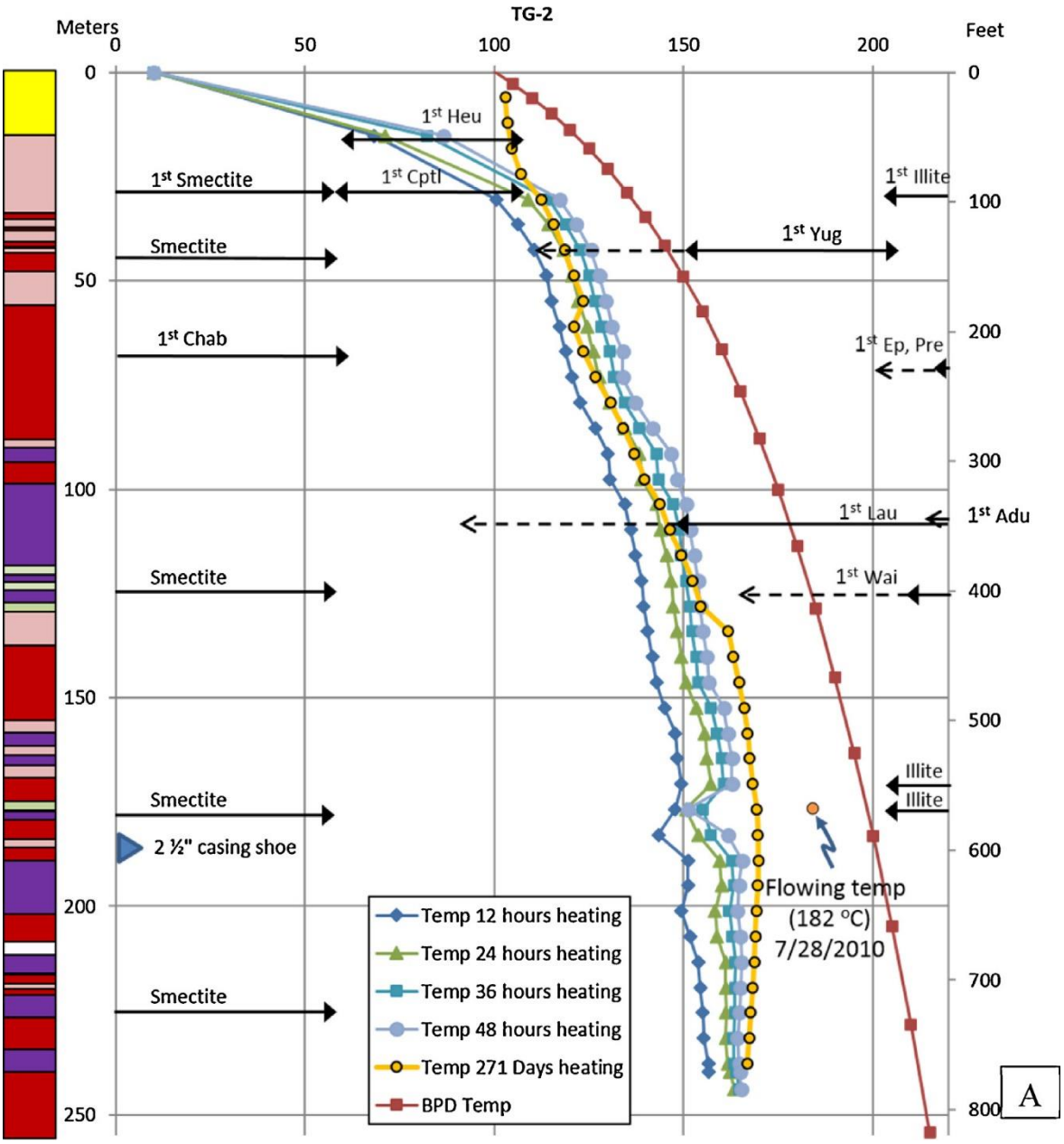

Figure 16: TG-2 well profile data from thermal gradient wells, including end-of-drilling temperatures, equilibrated temperatures (in C), lithologic column (left side; legend in center of (b)), occurrences of smectite clay identified during core analysis, and shallowest occurrence of important secondary minerals. BPD = Boiling point-depth curve.

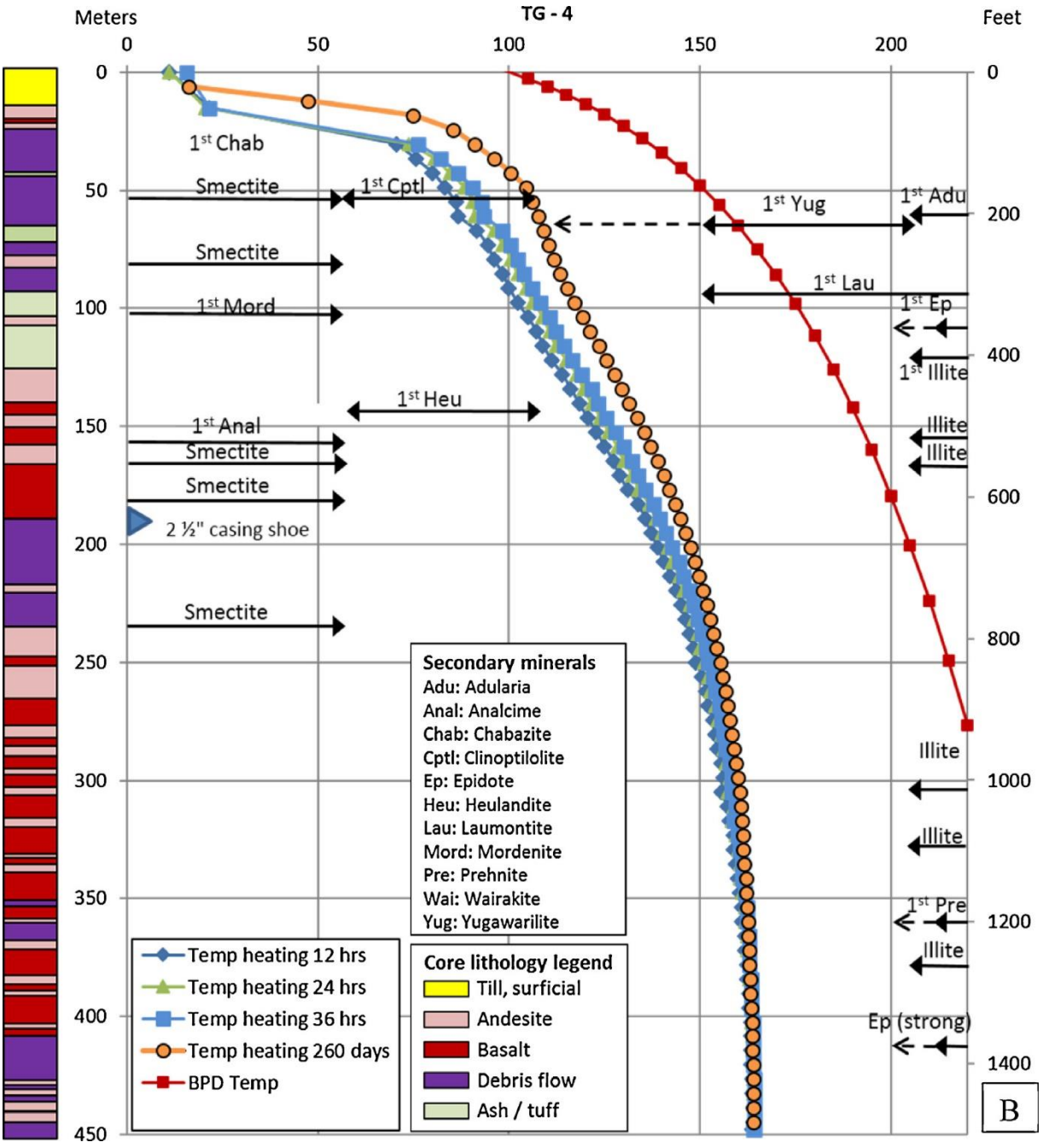

Figure 17: TG-4 well profile data from thermal gradient wells, including end-of-drilling temperatures, equilibrated temperatures (in C), lithologic column (left side; legend in center of (b)), occurrences of smectite clay identified during core analysis, and shallowest occurrence of important secondary minerals. BPD = Boiling point-depth curve.

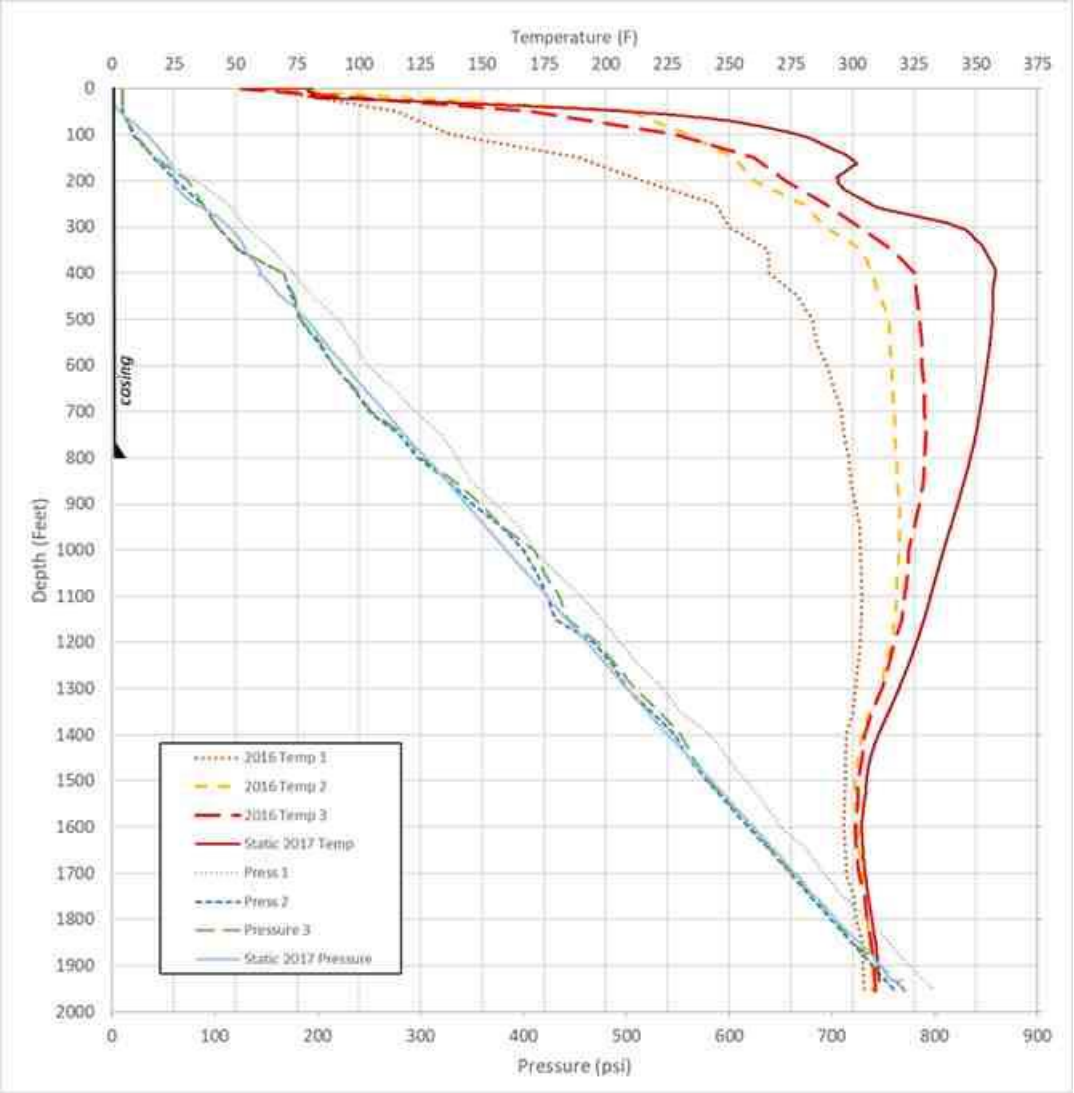

Figure 18: Static Pressure Temperature surveys from AK-3, heat up after drilling in 2016 and equilibrium prior to well testing in 2017.

Core Data

Lithology

There are three generalized lithologies present in the Akutan core (lava, tuff, and mass wasting deposits), all of which are expected based on the tectonic setting. All igneous samples contain some amount of plagioclase and groundmass glass; other primary constituents (e.g., pyroxene and olivine) appear to be less common. Basalt and andesite lava flow deposits make up 50-66% of the lithology of the core. Shallow recovery of scoria in AK-3 at 5’ and 7-8’ was the first occurrence

of scoria in any of the HSBV wells. The clay-rich sections in the top 20' are likely glacial and from increased rock breakdown as a result of the modern swampy conditions at the surface (although clay composition cannot be determined without further analysis).

Basalt and Andesite Lava

Basalt and andesite lava flows[1] appear to be subaeriallydeposited, but some flows may have a submarine origin (although no pillow basalts have been observed) and some may be peperitic (flowing from land into the sea, burrowing beneath unconsolidated marine sediment as it advances into the water). The composition of these rocks varies from a microcrystalline lava flow deposit with plagioclase and clinopyroxene pheonocrysts to sparsely phyric, plagioclase-bearing lavas.

Plagioclase phenocrysts are ubiquitous, and phenocrysts of mafic minerals (presumably clinopyroxene and olivine) are much less common, and possibly absent in the andesite. The tops of individual flows are identified by larger vug size and abundance. As a result of the increased porosity near the flow tops, they tend to be more altered and more readily brecciated than the main body of the flow. Contacts tend to be highly irregular and undulating, possibly reflecting rubbly flow tops.

Ash Tuff

Ash tuffs are very fine-grained rocks that generally lack prominent phenocrysts of any type. Groundmass phases are plagioclase microlites, glass, and alteration minerals. Tuff ranges from darker gray (interpreted to be relatively mafic) to light gray (interpreted to be andesitic or dacitic). Basal contacts are typically sharp and irregular, and all contacts appear to be more altered. The groundmass tends to be variably reactive to hydrochloric acid (HCl), suggesting pervasive alteration due to matrix flow throughout most units. Tuff units are commonly veined with 0.5-2 mm-wide calcite-dominated veins. In AK-3, tuff units range from 0.5' thick to ~64' thick, generally thicker than those observed in TG-2 cores and comparable to those observed in TG-4. Thinner units may be clasts contained within mass wasting deposits.

Mass Wasting Deposits

A variety of mass wasting deposits are observed in the HSBV core. These units are variably termed lahar, mass wasting, debris flow or lithic basalt. The latter term was derived during the drilling of TG-2 and TG-4, when a mass wasting deposit apparently had basaltic lava as the matrix. These

[1] The distinction between basalt and andesite in the field is largely based on lighter colored groundmass in andesite, which is not necessarily a valid compositional indicator. Mineralogically, these lithologies are very similar, with the mafic minerals generally more common in basalts. For the purpose of this report, and due to the ambiguity between basalt and andesite in field observation, they have been grouped together in this discussion.

deposits are likely representative of mass wasting with abundant microgranular basaltic sediment in the matrix. Deposits can be clast-supported or matrix-supported, angular, rounded or sub-rounded clasts, heterolithologic or homolithologic. Clast sizes can vary from silt-sized particles to >3' intermediate diameter.

Unit Correlation

Direct lithologic correlation between any of the three HSBV wells is difficult. This is due to several factors: (1) these are largely surficial volcanic (lava flows) and volcaniclastic (mass wasting) deposits that are likely to have restricted horizontal distribution so the likelihood of encountering the same deposit in two different wells is low; (2) none of these deposits have unique characteristics, making them nearly impossible to distinguish from other similar units in the stratigraphic sequence; and (3) until it is possible to directly compare the rocks from physical samples, interpretations of different lithologies based on descriptions from a different field geologist are subject to uncertainty. That said, the lithology encountered in all the wells is similar. Alteration in shallow portions of AK-3 is very similar to that observed in TG-2, except for a narrow zone of what appears to be intense alteration along a fracture network at 168-170'. This is likely the depth that produced the uncontrolled flow during drilling. Well TG-2 encountered a broad fracture zone at 588-590', with significant mud losses and permeability. A similar zone at this depth was not encountered in AK-3. Thus, the flow zone may only occur on one side of the fault presumed to exist between these wells.

Permeability

The matrix permeability of lithologies encountered in the HSBV wells are likely to be low. In wells TG-2 and TG-4, the permeability of lava flows is low, with tuffs and mass wasting deposits having slightly greater matrix permeability. Secondary mineralization along clast margins in some mass wasting deposits indicates that fluid flow through this lithology has been directed around clast boundaries in the past. Higher permeability appears to be generally restricted to the upper 900' of AK-3. In the shallow portions of TG-2 and AK-3 the fracture zones are within the mass wasting deposits. Most fractures in andesite and tuff appear to be sealed with secondary mineralization, suggesting these were fluid pathways in the past but do not appear to have significant permeability now.

Figure 19: Example of core from AK-3 from ~168' showing an apparent flowing fracture.

Alteration

Alteration is dominated by moderate propylitic alteration occurring in at least two different episodes evidenced by the presence of chlorite, zeolites, epidote, prehnite, pyrite, hematite, quartz and calcite.

The presence of clays is an important aspect of geothermal systems, with smectite clays helping to form a low-permeability clay cap, and high-permeability illite and chlorite clays forming regions of higher permeability. Smectite, illite and mixed-layer clays occur sporadically throughout the core, primarily along fracture margins and lithologic contacts. No thick zones of intense clay alteration were observed, although alteration is more intense in ash-fall tuff units and some mass wasting deposits. Smectite occurs at a depth of about 100 to 800 ft, often associated with fine-grained rocks. Illite occurs throughout the core, including at shallow depths (397 ft. (121 m) in TG-4 and 121 ft. (37 m) in TG-2; Figure 16, Figure 17). (Clay species indicated through X-Ray Diffraction analysis of samples from TG-2 and TG-4.) The localized presence of kaolinite indicates argillic alteration with lesser extent and lower intensity. The lack of abundant clay alteration suggests that permeability at depth in the HSBV system is less than excellent, as the circulation of hot fluids would produce more clay alteration at the top of the system. In order for a geothermal system to exist under HSBV, it would need to have a fairly robust seal that includes abundant clays.

The first occurrence of epidote is significantly shallower than the modern system could support. The in-situ formation of illite, adularia and epidote are also shallower than is possible in modern conditions. The alteration occurred when pressure was much higher than current hydrostatic from surface, implying either erosion of overlying rock or increased hydrostatic pressure due to overlying ice, or both. Thus, much of the propylitic alteration observed in the core does not reflect the modern hydrothermal system but rather an older, hotter system under greater pressure. This may positively impact permeability conditions in wells, as propylitic alteration tends to promote permeability due to the brittle nature of chlorite and illite clays regardless if these minerals were formed recently or in the past. The ubiquitous presence of calcite may be the result of recharge fluids moving through the system.

Conceptual Model Updates

The geologic mapping and expanded MT coverage in 2012 support upflow beneath the fumarole area and a lithologically and structurally controlled outflow that feeds the hot springs near the mouth of HSBV. These two distinct areas have very different surface manifestations, alteration mineralogy, fluid chemistry, temperatures and permeabilities. These two areas provide separate potential resource areas with different associated risk factors as discussed separately.

Hot Springs Resource Area

The absolute path of the outflow is less constrained, but it appears to flow broadly to the NE from the fumarole beneath Mount Formidable based on MT resistivity patterns, alteration patterns, surface expressions and measured spring temperatures. The broad MT resistivity patterns suggest this portion of the outflow is lithologically controlled, and relatively abrupt margins of resistivity patterns at the margins of the outflow suggest structural controls as well. The two flow paths suggested by Kolker et al., (2012) represent the southern and northern margins, respectively, of a more widely spread outflow.

The southern flow margin appears to be controlled by NW/SE structures parallel to the upper portion of HSBV and perpendicular to the main valley. These structures extend from the fumarole field to the juncture with the main valley, where fluid flow is apparently diverted NE along structures that form the northern margin of the main HSBV. Fluids travel parallel to the valley wall until they intersect cross-valley faults that cause the fluid to ascent, forming the chain of hot springs.

The northern flow margin is less rigidly constrained but likely involves lithologically-controlled fluid flow from the upflow to the ENE to the north of Mount Formidable until these fluids encounter a series of NW/SE trending structures parallel to those forming the southern flow

boundary at the head of the valley. Fluids are diverted to the SE to the intersection of these cross-valley faults and the valley-parallel faults of the southern flow boundary. Based on MT resistivity, it does not appear that the outflow is significantly deeper than 200 m below sea level (up to 300 m below the surface) along the cross-valley faults (Figure 22) or that the outflow extends significantly beneath the floor of HSBV toward the center of the valley. MT low-resistivity patterns extend NE across the NW/SE trending faults, suggesting these structures are not impermeable boundaries. The extent to which these structures allow fluid flow across them is the greatest source of uncertainty in the estimates of outflow resource volume and the risk associated with development of this resource.

The intersection of the northern and southern flow boundaries (fault zones) is located near the hot springs. It is likely that the valley-parallel and cross-valley structures exhibit sufficient control over fluid flow that a portion of the outflow fluids are forced to daylight in this area. Within the margins of the outflow, however, fluid flow appears to be distributed through lithologic units. The relatively high MT resistivity signatures in this area (>10 ohm-m) may result from fluid flow and alteration within several-meter-thick permeable lithologies bracketed by relatively impermeable (i.e., unaltered) units, resulting in a high average resistivity signature. The distributed and lithologically controlled fluid flow suggests that the greatest probability of exploration success will occur where fluid flow has been concentrated (e.g., near the hot springs area). Additional wells located further up-valley on the valley floor and directly north of Mount Formidable are less likely to encounter high fluid flow rates. Wells drilled NW of the hot springs, on top of the bench that forms the NW valley wall, are more likely to encounter higher fluid flow (Figure 20)

Because much of the data suggest low permeability conditions in the outflow portion of the HSBV, producing the outflow resource entails more risk. In addition to the well behavior and alteration patterns observed in the core discussed above, there is no well-developed clay cap to indicate that a large, very permeable reservoir volume at 180-220 °C exists under HSBV. The lack of widespread surface alteration, geochemical, and ground temperature anomalies (Kolker and Mann, 2009; Kolker et al., 2012; Stelling et al., 2015) in HSBV are consistent with this interpretation. Additionally, the chemical composition of the hot springs fluids suggests that outflow fluids become extensively mixed with cooler meteoric waters near the surface, raising concerns about cold water influx into the outflow system with production.

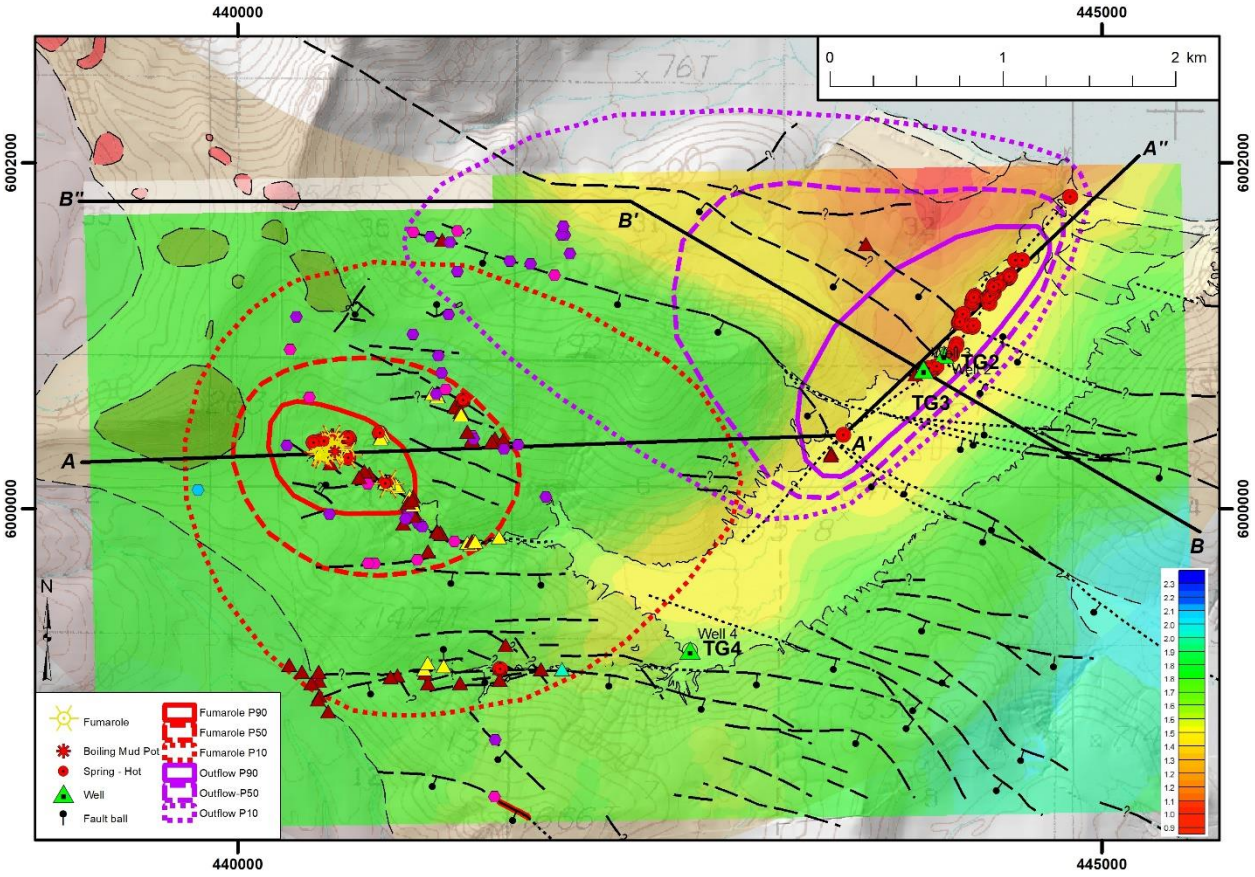

Figure 20: Map view of P90 (pessimistic; solid lines), P50 (median; dashed lines), and P10 (optimistic; dotted lines) probabilistic resource areas for fumarole and outflow parts of HSBV. Background MT resistivity slice at 100 m below sea level.

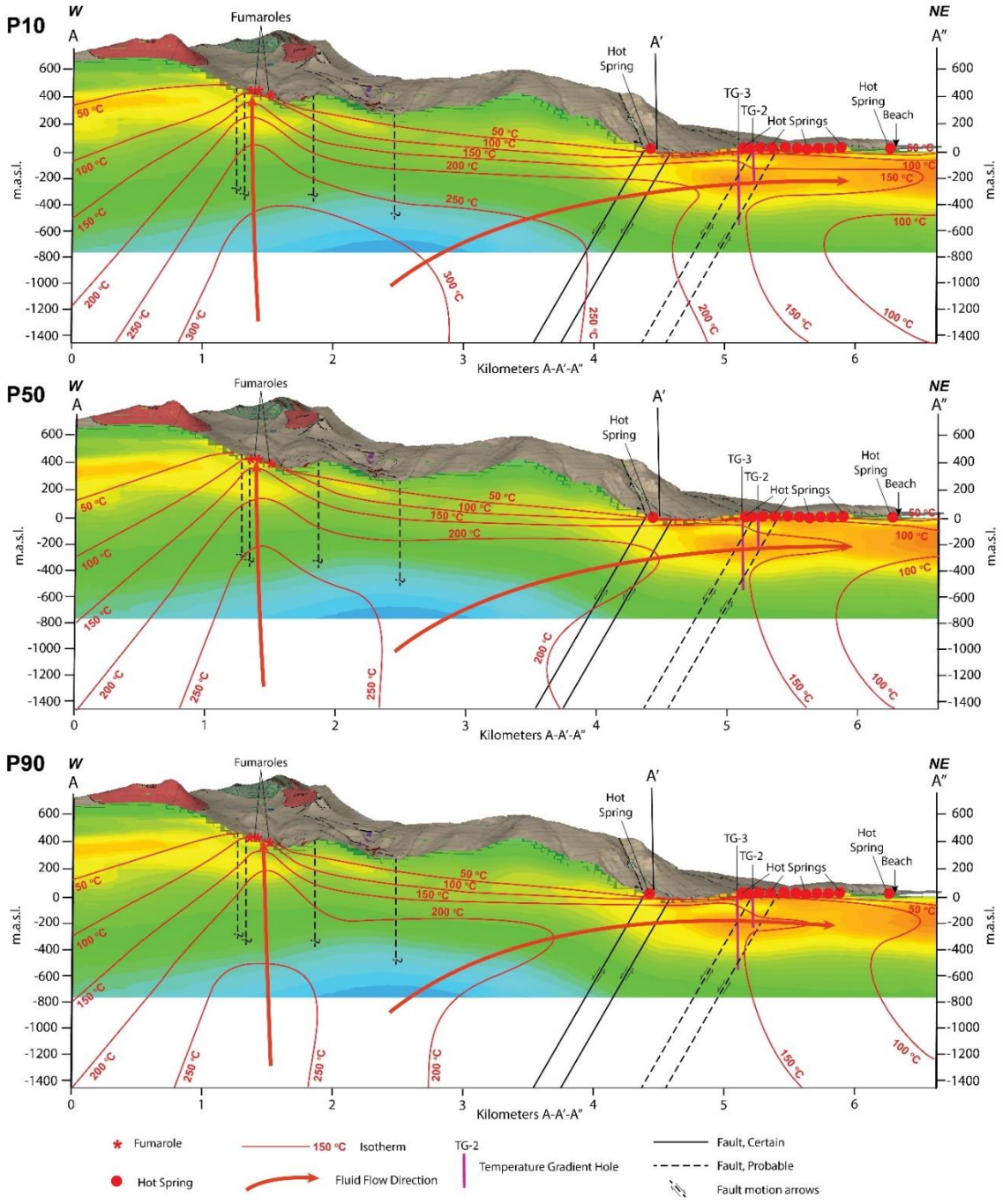

Figure 21: Valley parallel cross-sections of the P10 (optimistic; top panel), P50 (median; center), and P90 (pessimistic; bottom panel) probabilistic resource areas for fumarole and outflow resources of HSBV. Scale for MT resistivity background is the same as Figure 20.

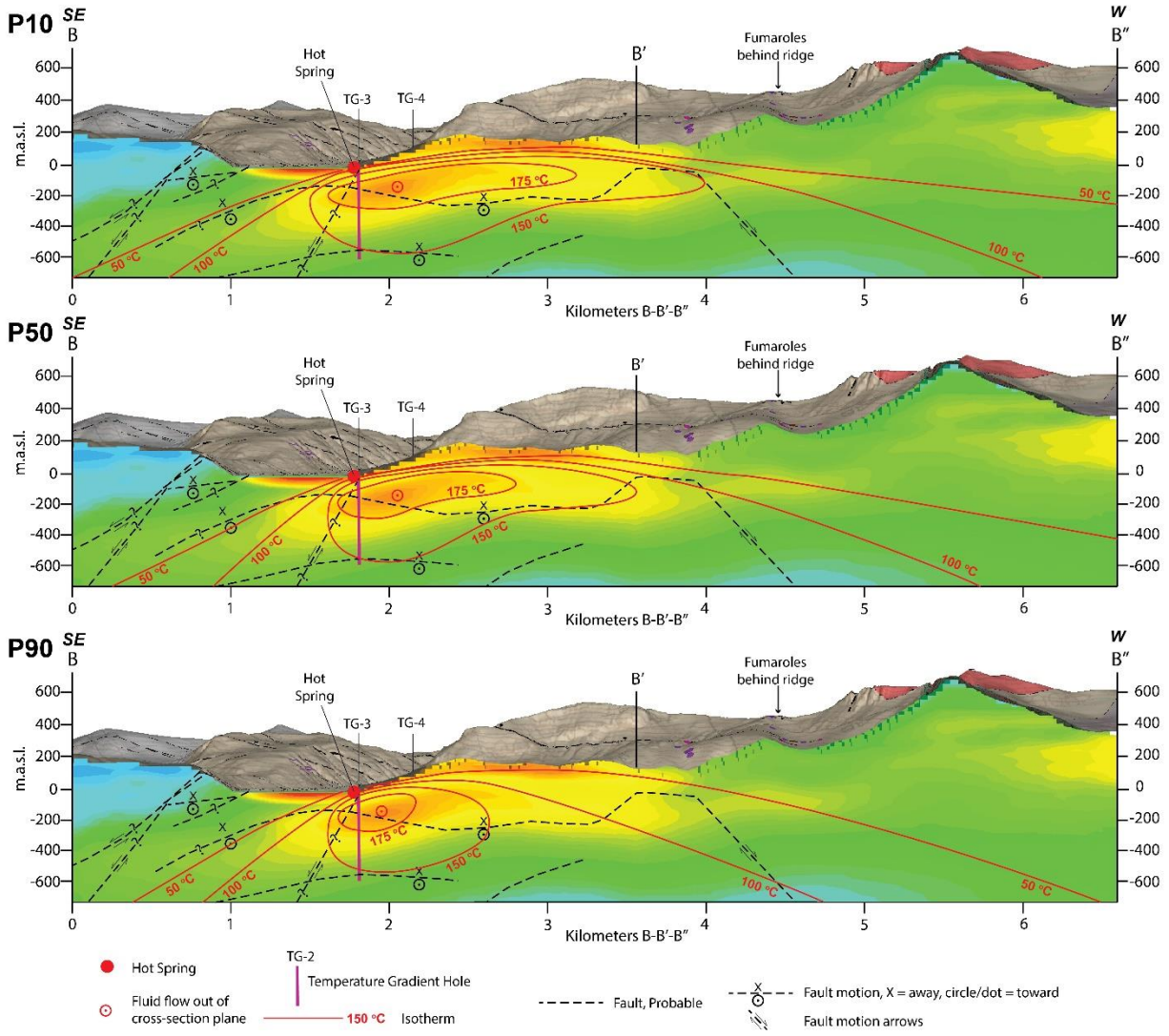

Figure 22: Valley perpendicular cross-sections, facing SW of the P10 (optimistic; top panel), P50 (median; center panel), P90 (pessimistic; lower panel), and probabilistic resource areas for fumarole and outflow resources of HSBV. Scale for MT resistivity background is the same as Figure 20.

Fumarole Resource Area

The area of greatest geothermal potential at HSBV is in the upflow zone near the fumaroles at the head of HSBV. Geochemical data from the fumaroles suggest that a deep reservoir is present that probably consists of a brine liquid capped by a small two-phase region (steam cap) with temperatures approaching 570 °F (300 °C). Resistivity data suggest that the upflow reservoir is situated in brittle rocks, implying propylitic alteration regime and a good possibility of high

permeability. The new mapping revealed a previously unrecognized an area of dense, overlapping, fault, fracture, and dike orientations (NE-, NW-, and E/W), another potential indicator of high permeability. The extent of surface alteration in the valleys east and south of the fumaroles suggest a range of possible reservoir sizes, which is the basis of the majority of the variation between P10, P50 and P90 resource areas (Figure 20). Estimates of producible reservoir temperatures are as high as 300°C and have a lower limit of ~170°C. This lower limit is within the range of producible temperatures in the outflow zone; however, it is likely that these temperatures exist in the clay cap portion of the upflow and therefore would have permeability values too low for production.

Geochemistry of fumarole gases and fluids suggest that the fluids present are likely near neutral pH, an important characteristic of productive geothermal systems. Mineralogy associated with the fumaroles include smectite clays with minor kaolinite, and minor to trace native sulfur deposits. This mineral assemblage is consistent with near-neutral fluids.

Resource Capacity Estimation

There are a variety of ways to estimate resource capacity in geothermal systems. Heat-in-place estimates for geothermal systems are common but often overestimate resource capacity by large factors, even orders of magnitude, due to unreasonably optimistic recovery factors (Grant, 2015). Power density estimates can often be as accurate as more complex heat-in-place estimates at the exploration stage as they rely on fewer assumptions and are calibrated against a large number of known operating fields (Wilmarth and Stimac, 2015).

A power density estimate was made for each of the two HSBV resources. The intent of the power density approach is to account for the uncertainty of the resource by estimating the most optimistic values (P10, or a 10% probability that the resource is that large) and the most pessimistic values (P90, or a 90% probability that the resource is at least that large) and creating a statistical average estimate for power capacity (P50). The estimates have been made using the worksheet provided by Cumming (2016) which assumes log-normal distributions between P10 and P90. These estimates use the map area (km^2) of the reservoir size, the estimated maximum and minimum reservoir production temperatures (°C) and an assumed average power density (MW/km^2). The aerial extent of the productive resource is obtained from interpretation of the conceptual model (Figure 20, 21, and 22). The maximum and minimum temperature estimates are based on measured temperatures and fluid and gas geothermometry. The estimated power density is derived from the power densities associated with 80 operating geothermal systems worldwide (Figure 23), which provides a range of power densities based on the minimum and maximum reservoir temperatures.

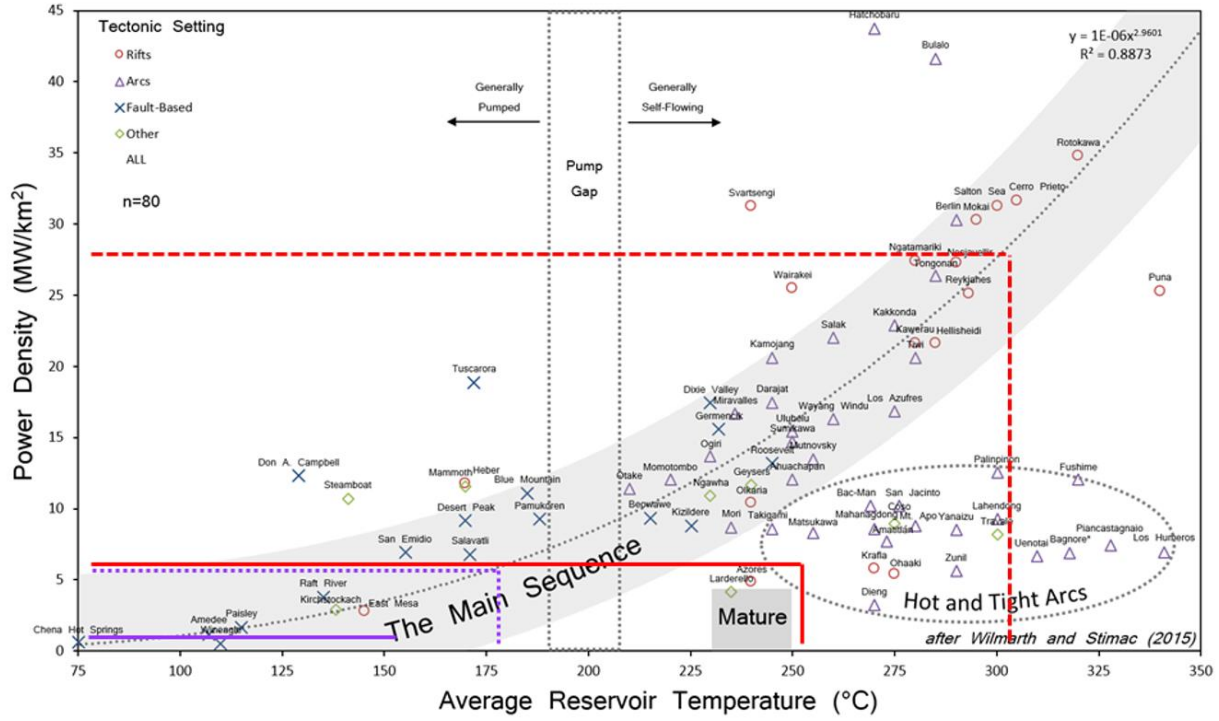

Figure 23: Power density plot of about 80 analog systems (Wilmarth et al., unpublished). Red lines correspond to temperature and power density ranges of the fumarole resource; purple lines correspond to temperature and power density ranges of the outflow resource. Dotted lines represent P10 (optimistic) values; solid lines represent P90 (pessimistic) values.

Fumarole Resource Power Capacity Estimates

The resource areas for both the fumarole and hot springs resources were based on the fumaroles, existing wells, hot springs, MT, alteration patterns, and distribution of faults, all of which has been incorporated into the conceptual model of the HSBV. Based on these factors, the fumarole resource has a production area between 0.24 (pessimistic, or P90) and 3.8 (optimistic, or P10) sq. miles (0.4 and 6.4 km^2). These areas are elongate to the SE due to the influence of the observed surface faults.

Geothermometry of the fumarole area ranges from ~250 to 275°C, possibly up to 300°C. Therefore, an estimated temperature range of 250-300°C was used. This corresponds to an expected power density range of 6-19.2 MW/sq. mi (10-32 MW/km^2; Figure 23). Many of volcanic systems in these temperature ranges have 3-6 MW/sq. mi (5-10 MW/km^2), but those with more favorable intra-arc tectonic setting can have greater power densities (Hinz et al., 2016). Specifically, the systems with the highest power densities in this range (Berlin, El Salvador; Mokai, New Zealand; Salton Sea, California, USA; Cerro Prieto Mexico) have a greater extensional tectonic component

than is observed at Akutan. Therefore, we have reduced the most optimistic resource density estimates (P10) to systems associated with more relevant tectonic settings. This reduces the optimistic value for the fumarole power density from 32/km^2 to 27 MW/km^2. A similar approach has been made for the pessimistic (P90) power density estimate, reducing this value to 3 MW/sq. mile (5 MW/km^2), which is consistent with analogous systems Zunil (Guatemala), Amatitlan (Guatemala) and Uenota, (Japan). The wide range is justified based on the active Quaternary faulting across the island, coupled with a moderately transtensional setting.

Hot Springs Resource Power Capacity Estimates

The hot springs resource is likely composed of one or more broad lithologic units with relatively high permeability with fault systems on the SE and NE margins that constrain and consolidate fluid. The highest concentration of hot fluid is likely to be near the intersection of these fault systems, near TG-2 and AK-3. The size of the resource is largely dependent on the volume of the more permeable units that extend from the fumaroles and beneath Mount Formidable, as well as how much fluid can penetrate the NW/SE trending fault system that crosses the lower HSBV. The estimates of resource area range from 0.6 to 3.8 sq. miles (1 to 6.4 km^2; Figure 20), with a mean area (P50) of 1.5 sq. miles (2.5 km^2).

The outflow resource has geothermometry values of 180°C and measured temperatures of 169°C. Thus, an estimated range of 150 to 170°C was used. As with the fumarole resource, the estimates for power density of the hot spring resource have been reduced from 6 MW/sq. mile (10 MW/km^2) to 3 MW/sq. mile (5 MW/km^2) based on the tectonic setting of analogous systems. The P90 (pessimistic) value has been maintained at 0.6 MW/sq. mile (1 MW/km^2).

Exploration Confidence Factors

The worksheet used for estimation handicaps undiscovered resources with exploration confidence factors for the probability of discovering commercial temperature, permeability and favorable reservoir chemistry. For the fumarole resource, temperature estimates are based on fluid and gas geothermometry with no measured subsurface temperatures. Accordingly, the confidence in obtaining reservoir temperatures >250°C (P_{Temp})has been estimated at 80%. Permeability is always the most challenging characteristic to predict, and a $P_{Permeability}$ of 65% was chosen, typical of other undiscovered resources at this stage of exploration in similar favorable structural settings. Reservoir chemistry in the fumaroles has several indicators of being benign and consequently a $P_{Chemistry}$ of 99% was chosen. The combination of these factors results in a probability of exploration success (POS_{expl}), the chance that at least one commercial well will exist) of 49%. With this handicap, the expected mean capacity is 20 MWe and the P50 (most likely) capacity is 9 MWe (Figure 24).

EXLORATION: Is it there?

Assuming a likely exploration geoscience program and drilling program, what is the percent confidence that at least one well is commercial

	Confidence in temperature.		Confidence in permeability. Commercial mDarcy		Confidence in chemistry. Not corrosive or scaling		Probability of exploration success
	PTemperature		PPermeability		Pchemistry		POSexpl
Exploration Confidence	80%	*	65%	*	95%	=	49%

APPRAISAL AND DEVELOPMENT: Assuming it's there, how big is it?

Cumulative confidence of representative optimistic case = **10%** That is, the larger, more optimistic case is assumed to be P10

Temperature range of permeable reservoir area from resource conceptual model. This should be consistent with assumed power density distribution.

Startup average production temperature for P90 reserves = **275** °C **275** °C = minimum temperature for P10 reservoir

Nu and Sigma are the mean and variance in log units required for specifying lognormal distributions in tools like @RISK

Representative Cases		P99	P90	Pessimistic P90	Middle P50	Optimistic P10	P10	P01	Mean	nu	sigma
Area > 275°C	**(km^2)**	0.1	0.4	**0.4**	1.6	**6.4**	6.4	19.6	2.9	0.46608	1.07867
Power Density 275 to 275 °C	**(MWe/km^2)**	2.5	5.0	**5.0**	11.6	**27.0**	27.0	53.7	14.4	2.45264	0.65795
MWe Capacity		1.0	3.7	3.7	18.5	93.5	93.5	350.0	41.1	2.91872	1.26350

EXPECTED POWER CAPACITY RESERVES (based on analogous reservoirs used to assess confidence in power density and area)

Expected Mean Capacity = 20 MWe = [Probability of Exploration Success] * [Mean Capacity of Development Assuming Exploration Success]

Expected P50 Capacity= 9 MWe = [Probability of Exploration Success] * [P50 Capacity of Development Assuming Exploration Success]

Adapted from Cumming, W., 2000. Spreadsheet for geothermal resource capacity scoping using lognormal area and power density distributions. Proprietary course material.

Figure 24: Power capacity calculation for the fumarole resource.

The probability of exploration success for the outflow resource is similar to that of the upflow. Measured temperatures are consistent with geothermometry results, allowing a P_{Temp} of 100%. Measured fluid chemistry is benign, allowing a Pchem of 95%. Production-grade permeability is a larger concern in the outflow, as drilling and testing results to date have not confirmed sustainable commercial flow rates. Thus, a P_{Perm} of 45% was chosen. This yields a POS_{expl} of 43%. Thus, the mean power capacity of the outflow resource is 3 MWe and the P50 (most likely) power capacity is 1 MWe (Figure 25).

EXLORATION: Is it there?

Assuming a likely exploration geoscience program and drilling program, what is the percent confidence that at least one well is commercial

	Confidence in temperature.		Confidence in permeability. Commercial mDarcy		Confidence in chemistry. Not corrosive or scaling		Probability of exploration success
	PTemperature		PPermeability		Pchemistry		POSexpl
Exploration Confidence	100%	*	45%	*	95%	=	43%

APPRAISAL AND DEVELOPMENT: Assuming it's there, how big is it?

Cumulative confidence of representative optimistic case = **10%** That is, the larger, more optimistic case is assumed to be P10

Temperature range of permeable reservoir area from resource conceptual model. This should be consistent with assumed power density distribution.

Startup average production temperature for P90 reserves = **150** °C **170** °C = minimum temperature for P10 reservoir

Nu and Sigma are the mean and variance in log units required for specifying lognormal distributions in tools like @RISK

Representative Cases		P99	P90	Pessimistic P90	Middle P50	Optimistic P10	P10	P01	Mean	nu	sigma
Area > 170°C	**(km^2)**	0.5	1.0	**1.0**	2.5	**6.4**	6.4	13.6	3.3	0.92815	0.72424
Power Density 170 to 150 °C	**(MWe/km^2)**	0.2	0.5	**0.5**	1.6	**5.0**	5.0	12.8	2.4	0.45815	0.89836
MWe Capacity		0.3	0.9	0.9	4.0	17.6	17.6	58.6	7.8	1.38629	1.15394

EXPECTED POWER CAPACITY RESERVES (based on analogous reservoirs used to assess confidence in power density and area)

Expected Mean Capacity = 3 MWe = [Probability of Exploration Success] * [Mean Capacity of Development Assuming Exploration Success]

Expected P50 Capacity= 1 MWe = [Probability of Exploration Success] * [P50 Capacity of Development Assuming Exploration Success]

Adapted from Cumming, W., 2000. Spreadsheet for geothermal resource capacity scoping using lognormal area and power density distributions. Proprietary course material.

Figure 25: Power capacity calculation for the outflow resource.

Resource Capacity Assessment

The Akutan resource is an identified resource and a reservoir engineering assessment of the reserves is warranted. Confidence is internalized in this assessment and is not external as in the exploration factors. The Akutan geothermal system is a single resource with surface manifestations that are 4 km apart. That alone, using a more traditional means of resource capacity estimation based on areal extent and thickness of the resource, assuming even minimal width, would put a potential reserve at over 40 MWe for the field. Using the geophysical and well data gathered over the last ten years, a better estimate would be 62 MWe (P10 number) for the entire resource (including under Mount Formidable). However, there are only 3 slimhole wells in field, and only two are into the reservoir. Both wells are near the hot springs, which is in the outflow plume and are low in temperature (165˚C). AK-2 did flow at a higher temperature (180˚C), but had to pull the fluids into the well, most likely along a fault. This does not indicate a large reservoir volume. Based on the linear line of hot springs they also look fault fed. Trying to develop in the valley along the hot springs appears to able to support only at 4 MWe (P90) maximum development, most likely 2 MWe (P50). Further exploration chasing the outflow plume backwards could increase the output to 9 MWe (P10), but that appears to be up west up the mountain and is not defined well and will require additional exploration and additional unproductive wells defining this outflow plume.

Development at the fumarole site is more understood, based on drilled geothermal systems in volcanic areas, and has a much higher likelihood of drilling useful productive wells from the outset.

It would also have a high likelihood of getting a minimum of 240˚C fluid, with likely 270˚C fluid and potential to 300˚C based on geochemistry. Given the known extent of the resource, it is very likely over 11 MWe (P90) would be able to be developed. It is most likely that over 20 MWe (P50) of high temperature fluids could be developed in this area. Wells in this area would provide over twice the energy per well that the hot springs wells would (need half the number of wells) and have a larger choice of more efficient plant options with the hotter fluids. Excess fluid could be flowed via pipeline for direct use applications allowing for some heat loss. If successful, development could possibly yield up to the P10 generation of 62 MWe, if other uses were found, although it would have chased the outflow back to the hot springs and lower temperatures. With higher potential there is less risk of obtaining the desired generation level or outgrowing the maximum generation level.

Resource Capacity Summary

Based on three methods of reserves estimation: Power Density, Exploration Confidence, and Reservoir Assessment, the fumarole area has a range of 3.7 MWe to 62 MWe with the optimistic (P90) number around 6 MWe and a most likely (P50) being 19.25 MWe. For the outflow area the range is 1 to 4 MWe for development along the hot springs, and 2 to 17.6 if additional development up the mountain from the hot springs in also developed. Most likely, the outflow area has a P50 value of 4 MWe considering all methods.

Resource Risks

Permeability is the greatest source of uncertainty in geothermal exploration, and the HSBV geothermal system is no exception. The hot springs resource area has been flow tested with moderate results, suggesting that commercial-grade permeability may be challenging to find. This represents the greatest exploration risk for the hot springs resource. For the fumarole resource, there is a greater likelihood of commercial-grade permeability based on the enhanced structural complexity apparent at the surface and apparent flow rates from the fumaroles.

The clay cap at HSBV appears to be rather sparse. MT resistivity signatures of <10 ohm-m, typical of most productive geothermal systems, is absent across HSBV. This may be the result of high permeability lithologic units (and therefore fluid flow and subsequent alteration) bracketed by low permeability lava flows with higher resistivity providing an elevated average resistivity value. Evidence from the drill core generally supports this idea, with fine-grained ash fall deposits and other units being much more altered and higher permeability than lava flow units. It is also possible that a more robust clay cap existed in the past and has since been partially eroded, likely by glaciation. This is supported by the occurrence of high temperature alteration minerals occurring at surprisingly shallow depths in the core. The lack of a well-developed clay cap limits

the expectations of a highly pressured system. These characteristics have been incorporated into the conceptual model and the resource capacity calculations.

Project Feasibility-Next Steps

The Akutan geothermal resource can be divided into an upflow zone (fumarole area) and a broader outflow zone (hot springs area). Although the conceptual models of the hot springs resource have downgraded its development potential from initial expectations, geochemical and mapping data from the fumaroles has significantly upgraded the resource potential of the fumarole area. Studies of alteration minerals in the core suggest that the outflow region has reached a thermal maximum and is in a cooling phase, although fluid temperature and flux studies indicate an increase in both fluid flow and temperature between 1980 and 2012 (Bergfeld et al., 2014). The presence of an intermittent clay cap, high resistivity values, and high temperature minerals occurring at surprisingly shallow depths in the outflow region suggest the uppermost portion of the outflow region may have been eroded, possibly due to glaciation. Alteration and secondary mineralization in the outflow region have resulted in "self-sealing" of permeable structures, and the outflow resource discovered by TG-2 is likely to have significant permeability limitations. The peak outflow resource temperature of 359 °F (182 °C) discovered during exploratory drilling in 2010 appears to reflect fluid "pulled in" from a nearby source. The highest measured temperature in AK-3 was 358°F at 405'. A temperature reversal at the bottom of the stabilized AK-3 profile reduces the possibility that a hotter or more voluminous reservoir would be encountered by drilling deeper at that location. New geochemical data from well fluid and fumaroles indicates that the upflow region of the Akutan system, in the vicinity of the fumaroles, is >428-572 °F (220-300 °C), near neutral chloride system with minor volcanic affinity and a steam cap. Thus, the greatest probability of overall MWe production is in this region.

With data already collected additional interpretation that could help with future well targeting would be a 3D joint inversion of MT and gravity data, combined with modeling of oceanic influences. This would ideally be combined with 1D spot inversion of MT data for quality assurance. This will be important for the hot springs area in particular, where the MT data may have imprints of seawater influence.

The first well drilled into the fumarole (upflow) area will provide a lot of direct information on this reservoir and will have good probability for successful production. Wells drilled beneath the fumaroles will require infrastructure investments in the form of roads either to the floor of the head of the valley or, ideally, to the crest of the ridge west and southwest of the fumarole area. This

higher elevation will allow for additional distance to navigate a directionally drilled well into the upflow zone.

The next steps required for the project, to close the grants, and continue seeking ways to continue the program include, first determining the short-term plan for well AK-3. AK-3 permit is maintained at Alaska Oil and Gas Confirmation Commission (AOGCC) and to keep the well in its current suspension mode, a location survey as well as a wellhead inspection are required. The AOGCC can allow suspension for up to several years at a time, the current suspension is valid until 2020, with the indicated surveys. Abandonment of this well is not recommended at this time, as the next steps for the project are not yet determined and it may be useful to have access to the well for injection, monitoring or continued testing.

The fumarole site has more electrical generation potential than the hot springs site, and given the continued expansion of development on the island, including the harbor (electrification scheduled for Summer 2019), fish plant expansion, and the airport, it may be that development of this part of the geothermal resource is viable. An initial revision of the budgetary estimates from the aborted Phase 3 work, indicates fairly similar resource confirmation and production drilling costs as well as development estimates. Some cost savings could be realized using a track mounted rig, but the costs of access are significant. General planning budget baseline estimates do not include contingency and certain logistical costs, which are estimated as 30 percent of construction costs. The total development estimate is $45 million to $57 million, as broken out below:

- Per well drilling costs for a track mounted rig: $3.5 to $4 million per well (6,000-8,000 ft slim well suitable for production testing)
- Per well drilling costs for a 1000 HP rig: $6.4 million (6,000-8,000 ft well suitable for production)
- Infrastructure development (drilling pads, plant site, access road, water supply system): $8 to $9 million.
- Infrastructure development (setup for a 1000 HP rig including roads, drilling pad etc): $12 to $15 million
- Condensing steam plants-modular type (total of 10 MW): $20-24 million
- Transmission lines: $1.5 million to $2.5 million

Depending on investor interest there are as yet undefined opportunities to use the outflow resource for more direct use applications, to be explored. The City should continue to seek additional interest in development of the geothermal resource of HSBV through outside investment and additional grant opportunities.

References

Bergfeld, D., Lewicki, J.L., Evans, W.C., Hunt, A.G., Revesz, K. and Huebner, M. 2014. Geochemical Investigation of the Hydrothermal System on Akutan Island, Alaska, July 2012. U.S. Geol. Surv. Sci. Invest. Rep. 2013-5231, 20 p. http://dx.doi.org/10.3133/sir20135231.

Cumming, W., 2016, Resource Conceptual Models of Volcano-Hosted Geothermal Reservoirs for Exploration Well Targeting and Resource Capacity Assessment: Construction, Pitfalls and Challenges, GRC Transactions, Vol. 40, 16pp.

Geothermal Resource Group, 2012, Preliminary Summary of Findings Akutan Geophysical and Geological Investigation, For the Purpose of Delineating and Targeting the Geothermal Resource of Hot Springs Bay Valley, Commissioned by City of Akutan, Alaska

Geothermal Resource Group, 2014, Akutan Well AK-3 Drilling Site Selection Document, Prepared for City of Akutan, 14p.

Geothermal Resource Group, 2016, Akutan Geothermal Project AK-3 End of Well Report, 29 pp.

Geothermal Resource Group, 2017, Akutan Geothermal Project, Well AK-3 Flow Test Report, August 2017, 30 pp.

Kolker, A., P. Stelling, B. Cumming, A. Prakash, and C. Kleinholt, 2009. Akutan Geothermal Project: Report on 2009 Exploration Activities. Unpublished report to the City of Akutan and the Alaska Energy Authority, 37p.

Kolker, A., B. Cumming, and P. Stelling, 2010. Akutan Geothermal Project: Preliminary Technical Feasiblity Report. Unpublished report to the City of Akutan and the Alaska Energy Authority, 31p.

Kolker, A. Cumming, W., Stelling, P., Rohrs, D., 2011, Akutan Geothermal Resource Assessment, Commissioned by City of Akutan, 34p.

Kolker, A., Stelling, P., Cumming, W., & Rohrs, D., 2012. Exploration of the Akutan geothermal resource area. In Proceedings, Thirty-Seventh Workshop on Geothermal Reservoir Engineering (Vol. 37).

Kolker, A., B. Cumming, and P. Stelling, 2010. Geothermal Exploration at Akutan, Alaska: Favorable Indications for a High-Enthalpy Hydrothermal Resource Near a Remote Market. Geothermal Resource Council Transactions No. 34, 14p.

Hinz, N.H. and G. Dering, 2012. “Stratigraphic and Structural Controls of the Hot Springs Bay Valley Geothermal System, Akutan Island, Alaska.”, University of Nevada, Reno, Final Report, 28 pages.

Lu, Z., Wicks, C., Dzurisin, D., Thatcher, W. and Power, J., 2000. Ground Deformation Associated with the March 1996 Earthquake swarm at Akutan Volcano, Revealed by Satellite Radar Interferometry. Journal of Geophysical Research, v. 105, No. B9, p. 21483-21495.

Mira Geoscience, 2014, Rock Density and Gravity Data Analysis, 3D Geoscience Data Integration, and Interpretation at the Akutan Island Geothermal Project, Geothermal Resource Group, Inc., Project #4309, 37 pp.

Motyka, R., and Nye, C., eds., 1988. A geological, geochemical, and geophysical survey of the geothermal resources at Hot Springs Bay Valley, Akutan Island, Alaska. Alaska Division of Geological and Geophysical Surveys, Report of Investigations 88-3.

Ohren, M., A. Bailey, N. Hinz, G. Oppliger, J. Hernandez, W. Rickard, and G. Dering, 2013. “Akutan Geothermal Area Exploration Results and Pre-Drilling Resource Model.” Transactions of the Geothermal Resources Council, vol. 37, p. 301-307.

Powell, T., and W. Cumming., 2010. Spreadsheets for Water and Geothermal Gas Chemistry. Proceedings of the Thirty-Fifth Workshop on Geothermal Reservoir Engineering, Stanford University, Stanford, California, SGP-TR-188.

RMA Consulting Group, 2014, Phase III Progress Report, for the Period 1 September 2013 – 28 February 2014, Akutan Geothermal Development Project, Alaska Energy Authority, Grant Agreement Number 7040050

Stelling, P. and T. Kent, 2011. “Geological Analysis of Drill Core from Geothermal Gradient Wells HSB2 and HSB4.” Consultant report, Stelco Magma Consulting and Western Washington University, 24 pages.

Stelling, P., Kolker, A., and Cumming, W., 2010. Geoscientific Data Types used to Support Geothermal Exploration at Akutan, Alaska: An Analysis of Relative Effectiveness in Thermal Gradient Well Targeting. Abstract V23D-07 presented at 2010 Fall meeting, AGU, San Francisco, Calif., 13-17 Dec.

Stelling, P., N.H. Hinz, A. Kolker, and M. Ohren, 2015. “Exploration of the Hot Springs Bay Valley (HSBV) geothermal resource area, Akutan, Alaska.” Geothermics, vol. 57, p. 127-144.

Wilmarth, M. and Stimac, J, 2014, Worldwide Power Density Review, 39th Workshop on Geothermal Reservoir Engineering, SGP-TR-202, 5 pp.